Discovery of a novel lysophospholipid acyltransferase family essential for membrane asymmetry and diversity.

生体膜の非対称性および多様性に重要な
新規リゾリン脂質アシル基転移酵素ファミリーの発見

菱川 大介

Contents

Abbreviations

ACAT; acyl-CoA:cholesterol *O*-acyltransferase

AGPAT;
1-acylglycerol-3-phosphate-*O*-acyltransferase

ALCAT; lysocardiolipin acyltransferase

BSA; bovine serum albumin

CHO; Chinese hamster ovary

CL; cardiolipin

CDP-DAG; cytidine diphosphodiacylglycerol

CoA; coenzyme A

DAG; diacylglycerol

DHT; dihydrotestosterone

ECL; enhanced chemiluminescence

ER; endoplasmic reticulum

ESI-MS;
electrospray ionization mass spectrometry

FBS; feral bovine albumin

G3P; glycerol-3-phosphate

GPAT; glycerol-3-phosphate acyltransferase

GPI; glycosylphosphatidylinositol

MBOAT; membrane bound *O*-acyltransferase

LC-MS;
liquid chromatography-mass spectrometry

LPAAT; lysophosphatidic acid acyltransferase

LPCAT; lysophosphatidylcholine

LPEAT;
lysophosphatidylethanolamine acyltransferase

LPGAT; lysophosphatidylglycerol acyltransferase

LPIAT; lysophosphatidylinositol acyltransferase

LPLAT; lysophospholipid acyltransferase

LPSAT; lysophosphatidylserine acyltransferase

LysoPAFAT;
lyso platelet-activating factor acetyltransferase

PA; posphatidyc acid

PC; phosphatidylcholine

PE; phosphatidylethanolamine

PG; phosphatidylglycerol

PI; phosphatidylinositol

Pi; inorganic phosphate

PPi; inorganic pyrophosphate

RT-PCR;
reverse transcription polymerase chain reaction

siRNA; small interfering RNA

TAG; triacylglycerol

TEM; transmission electron microscopy

TLR; toll-like receptor

Summary

In addition to important structural and functional components of the cellular membrane, membrane phospholipids are important as a source of various lipid mediators. The fatty acid species in the membrane phospholipids are diverse depending on the polar head group of phospholipids and tissues. In glycerophospholipids, polyunsaturated fatty acids (PUFA) such as arachidonic acid or eicosapentaenoic acid, are located in an asymmetrical manner, being found at the *sn*-2 position of the glycerol backbone, but not at the *sn*-1 position. The asymmetrical properties of membrane phospholipids are important for membrane flexibility, fluidity and curvature. The rapid turnover of the *sn*-2 acyl moiety of glycerophospholipids was described in 1958 as a remodeling pathway, known as the Lands' cycle, and is due to the concerted activities of phospholipase A_2s (PLA_2s) and lysophospholipid acyltransferases (LPLATs). The exclusive presence of an unsaturated fatty acid at the *sn*-2 position of membrane phospholipids is maintained in the remodeling pathway. However, the molecular mechanisms and biological significance of this remodeling pathway have remained for a long time elusive. Here, I report the discovery of a new acyltransferase family called the membrane bound O-acyltransferase (MBOAT) family. Within this family, I identified three enzymes that catalyze the transfer of various types of acyl-CoAs to lysophospholipids to produce different classes of phospholipids. These enzymes showed different tissue distributions and substrate specificities; one termed lysophosphatidylcholine acyltransferase-3 (LPCAT3) prefers arachidonoyl-CoA, and the other 2 enzymes, which termed LPCAT4 and LPEAT1, incorporate oleoyl-CoAs

into lysophospholipids. Importantly, siRNA specific for LPCAT3 reduced endogenous LPLAT activities and the amount of phospholipids containing PUFA at the *sn*-2 position. Thus, I propose that the diversity of membrane glycerophospholipids is produced by the concerted and overlapping activities of multiple enzymes that recognize both the polar head group of glycerophospholipids and various acyl-CoAs.

Introduction

Tissues maintain distinct proportions of various phospholipids such as phosphatidic acid (PA), phosphatidylcholine (PC), phosphatidylethanolamine (PE), phosphatidylglycerol (PG), cardiolipin (CL), phosphatidylinositol (PI), and phosphatidylserine (PS) (1-3). The acyl groups of glycerophospholipids are highly diverse and are distributed in an asymmetrical manner. Saturated and monounsaturated fatty acids are usually esterified at the *sn*-1 position, whereas polyunsaturated fatty acids are esterified at the *sn*-2 position. This asymmetrical distribution of fatty acids is important for membrane flexibility, fluidity, and curvature. (4-6). In all cells, glycerophospholipids are produced from glycerol-3-phosphate (G3P), which is converted to lysophosphatidic acid (LPA) by G3P acyltransferase (GPAT) (7,8). Subsequently, LPA is converted to PA by LPA acyltransferase (LPAAT). PA is then metabolized into two types of glycerol derivatives, namely diacylglycerol (DAG) and cytidine diphosphodiacylglycerol (CDP)-DAG. Next, DAG is further converted to triacylglycerol (TAG), PC, and PE, and in some cases, into PS from PC or PE. In contrast, CDP-DAG, which is transformed into PI, PS, PG, and CL (9-11) (Fig. 1). This *de novo* pathway of glycerophospholipids synthesis is originally described by Kennedy in 1956, and is called the Kennedy pathway. Next, glycerophospholipids are matured in the remodeling pathway. Fatty acyl moieties at the *sn*-2 position are released by the activated PLA_2s, and subsequently reacylated by the action of lysophospholipid acyltransferases (LPLATs) (12-16) (Fig. 2). This remodeling cycle is proposed by Lands in 1958, and called Lands' cycle (17,18) (Fig. 2). Remodeling of the fatty acid in

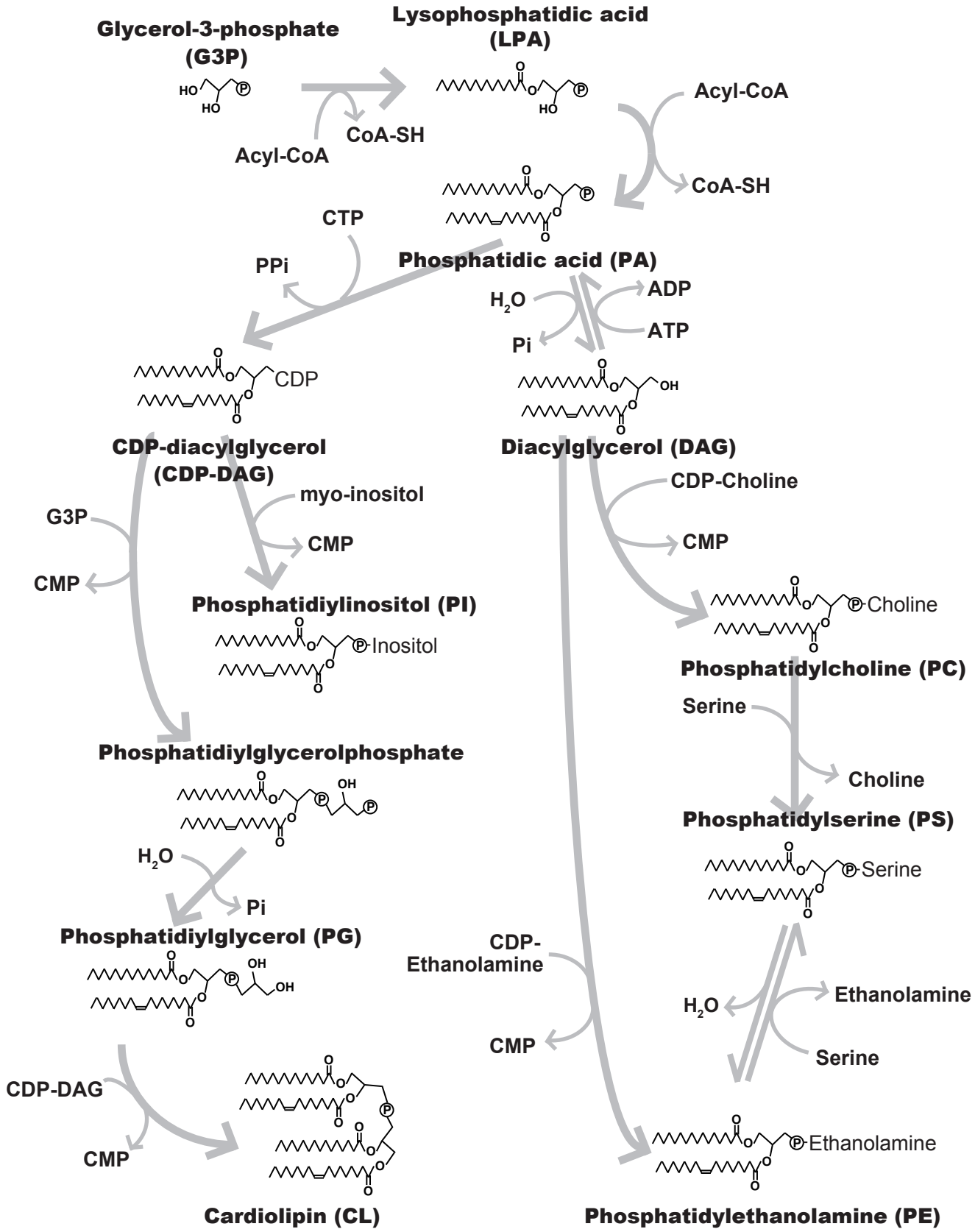

Fig. 1. The *de novo* pathway (Kennedy pathway) of phospholipid.
In mammalian cells, membrane phospholipids are synthesized from glycerol-3-phosphate through several steps. *See text for details.* Pi, inorganic phosphate; PPi, inorganic pyrophosphate, ADP, adenosine diphosphate; ATP, adenosine triPhosphate; CMP, cytidine monophosphate; CDP, cytidine diphosphate.

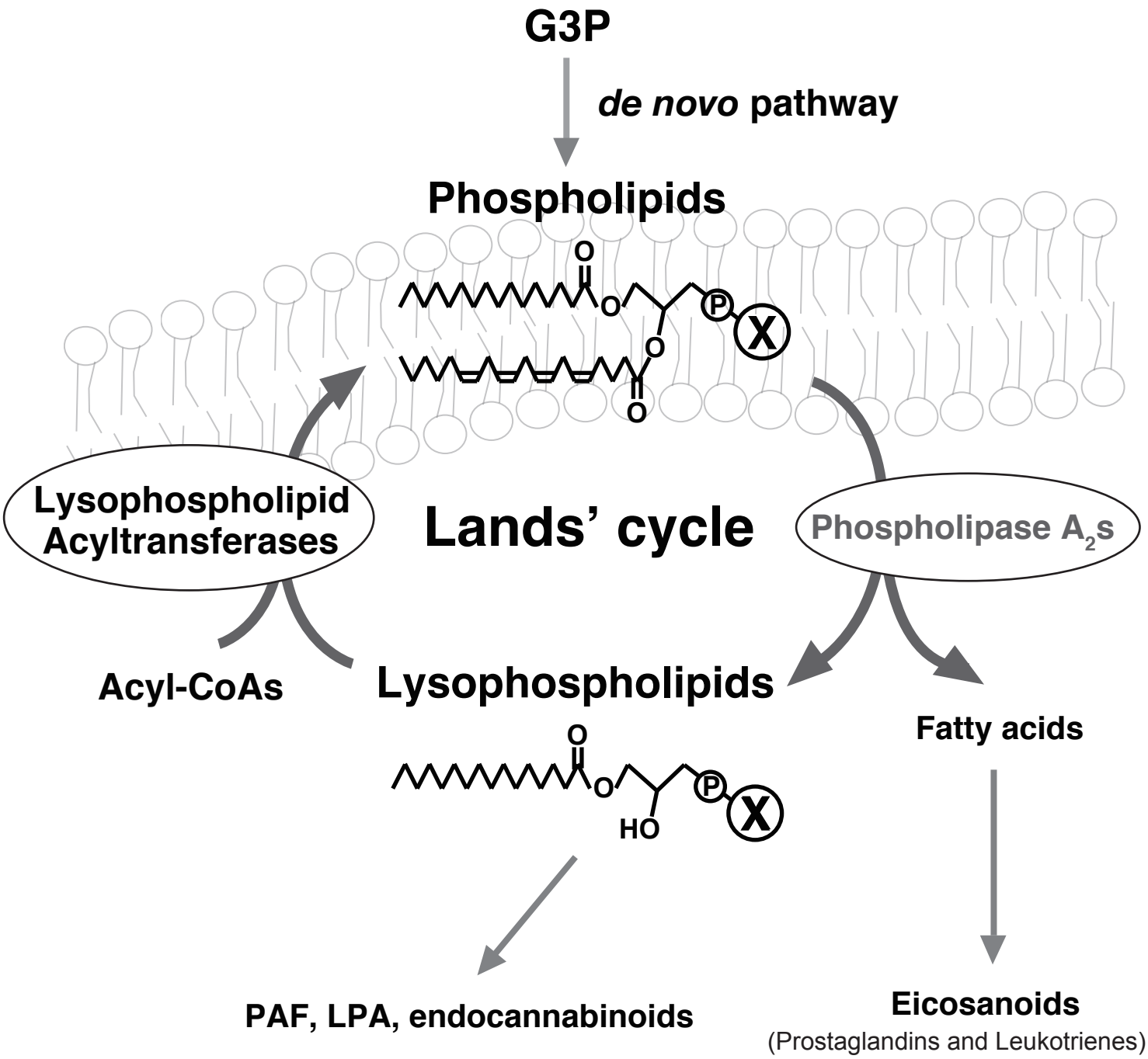

Fig. 2. The remodeling pathway (Lands' cycle) of phospholipid synthesis.
Fatty acids of phospholipid are liberated by PLA_2s and converted to eicosanoids such as prostagrandins and leukotrienes. Lysophospholipids are also lipid mediators such as LPA or precursors of a different class of lipid mediators including PAF and endocannabinoids. Lysophospholipids are converted to phospholipids in the presence of acyl-CoA by LPLATs. X indicates several polar head groups of phospholipids. *See text for details.*

the *sn*-2 position is important not only for the production of lipid mediators, such as lysophospholipid derivatives and eicosanoids, but also for the replacement of the oxidized unsaturated fatty acid with an unoxidized fatty acid (19-21). Although these metabolic processes are carried out in a variety of tissues, knowledge of the enzymes molecules involved in the reacylation of lysophospholipids is limited.

Previously, Kume and Shimizu in our laboratory cloned lyso-PA acyltransferase 1 (LPAAT1), and found that this enzyme used LPA solely as an acyl acceptor (10). While the recombinant LPAAT1 was shown to utilize various fatty acyl-CoAs as acyl donors, only LPA was found to serve as an acceptor. Several LPLATs including LPAAT1 and LPAAT2, lyso-PG acyltransferase (LPGAT) and lyso-CL acyltransferase (ALCAT), have been cloned in the last decade, and putative LPAATs (γ, δ, ε, ζ, and η) and tafazzin have been reported (22-29). Recently, our group newly identified two lyso-PC acyltansferases (LPCATs), designated LPCAT1 and LPCAT2, that function in the remodeling pathway and are mainly expressed in lung and inflammatory cells, respectively (30,31). These enzymes are members of the 1-acylglycero-3-phosphate acyltransferase (AGPAT) family and possess four well-conserved domains, designated motifs 1-4 (AGPAT motifs) (32), and an endoplasmic reticulum (ER) retention sequence (33) (Fig. 3A). Prior to the work presented here, there were no reports of mammalian lyso-PE acyltransferase (LPEAT), lyso-PS acyltransferase (LPSAT), or lyso-PI acyltransferase (LPIAT). Moreover, I believe that, in addition to LPCAT1 and LPCAT2, different LPCATs may exist for the purpose of membrane biogenesis, since PC biosynthesis in the Lands' cycle occurs in a

variety of tissues (34).

In this study, I identified a new family of LPLATs. The members of this new family have been previously reported as uncharacterized proteins, termed membrane bound O-acyltransferases (MBOATs) (35) that lack AGPAT motifs. Among these proteins, I found that mouse MBOAT1, 2 and 5 exhibited various LPLAT activities: (i) MBOAT1 has LPEAT and LPSAT activities; (ii) MBOAT2 has LPCAT and LPEAT activities; and (iii) MBOAT5 has LPCAT, LPEAT, and LPSAT activities. To avoid confusion, I refer to mouse MBOAT1, 2 and 5, as mouse LPEAT1 (mLPEAT1), mLPCAT4, and mLPCAT3, respectively, based on their characteristic properties.

To my knowledge, this is the first documentation of cDNAs being isolated for mammalian LPEAT and LPSAT, and the first report of the two additional LPCATs. Moreover, I functionally characterized MBOATs as a new LPLAT family. MBOATs are critically important remodeling enzymes for membrane phospholipids biosynthesis in the Lands' cycle.

Materials and Methods

Materials

Various phospholipids and acyl-CoAs were obtained from Avanti Polar Lipids (Alabaster, AL). Linoleoyl-CoA (C18:2) was purchased from Sigma. 1-*O*-alkyl-LPC (Lyso-PAF) was purchased from Cayman Chemical Company (Ann Arbor, MI). 1-*O*-alkenyl-LPC was from Doosan Serdary Research Laboratories (Toronto, Canada). [1-^{14}C]oleoyl-CoA (1.924 GBq/mmol), [1-^{14}C]linoleoyl-CoA (2.035 GBq/mmol), and [1-^{14}C]arachidonoyl-CoA (2.035 GBq/mmol) were purchased from Moravec Biochemicals (Mercury Lane, CA). [1-^{14}C]palmitoyl-CoA (2.22 GBq/mmol) was from GE Healthcare UK Ltd. (Buckinghamshire, England). TLC plates 20 x 20-cm (silica gel 60) were purchased from MERCK (MERCK Ltd. Japan). Phosphate buffered saline (PBS), Dulbecco's Modified Eagle Medium (DMEM), Nutrient Mixture F-12 (Ham's F-12), Roswell Park Memorial Institute Medium (RPMI 1640), and Iscove's Modified Dulbecco's Medium (IMDM) were purchased from Sigma-Aldrich (St. Louis, MO). MEM (Minimum Essential Medium Eagle), Alpha MEM (MEM alpha modification with ribonucleosides and deoxyribonucleosides), and fetal bovine serum (FBS) were purchased from Gibco Invitrogen Corporation (Grand Island, NY). Lipopolysaccharide from *Salmonella Minnesota* was purchased from Sigma-Aldrich. ODN1826 and poly(I:C) were purchased from InvivoGen (San Diego, CA).

Cloning of mLPCAT3, mLPCAT4, and mLPEAT1

The entire coding region of mLPCAT3 (DDBJ accession number, AB294194), mLPCAT4 (AB297383) and mLPEAT1 (AB297382) was amplified by PCR using DNA template from testis, stomach, and colon, respectively. The PCR products of each gene were amplified a second time, during which the FLAG epitope (DYKDDDDK) was attached to the N-terminus via modified forward primers during the second PCR. The amplified DNA fragments were each cloned into the pCXN2.1 vector (36) using multiple cloning sites, and sequenced. The primers used for cloning these enzymes are shown in Table 1.

Cell culture

MBEC4 (mouse brain capillary endothelial), MLE12 (mouse lung epithelial) LLC (Lewis lung carcinoma), Hepa1-6 (Non-immunogenic murine hepatocellular carcinoma), N1E (neuroblastoma), NIH-3T3 (mouse embryonic fibroblasts), SWISS-3T3(mouse embryonic fibroblasts), L929 (mouse connective tissue-derived fibroblasts), B16, B16F10, and B16BL6 (all three of these are mouse melanoma cells) cells were grown in DMEM with 10% FBS. Colon26 (mouse colon adenocarcinoma), and RAW264.7 (mouse leukaemic monocyte macrophage) cells were grown in RPMI with 10%FBS. Mouse epididymis-derived PC1, DC1, and DC2 cells were grown in IMBM supplemented with 10% FBS, 1 mM sodium pyruvate, 0.1 mM non-essential amino acids, 4 mM L-glutamine, and 1 nM 5-alpha DHT. Neuro2a (mouse neuroblastoma) cells were grown in MEM supplemented with 10% FBS and 0.1 mM

Table 1

Primers used in this study

Primer name	Sequence (5'-3')	Product size (bp)
Primiers for cDNA cloning of mLPCAT3, mLPCAT4, and mLPEAT1		
mLPCAT3-1stPCR-F	AATTGGGGGTGAAGCCAC	
mLPCAT3-1stPCR-R	AGGAGTGCTGTGAGAAGGGA	1617
mLPCAT4-1stPCR-F	TAGAACGTAGCTCGGCACAG	
mLPCAT4-1stPCR-R	AGGCCTCAAGACTGGCTTCT	1637
mLPEAT1-1stPCR-F	CGACAGAGCACCCTGAAGAT	
mLPEAT1-1stPCR-R	GTCCCGCAACTCTCTTGTTC	1542
FLAG-mLPCAT3-2ndPCR-F	CTAGCTAGCCACCATGGATTACAAGGATGACGATGACAAGGCGTCTACAGCGGACGGGG	
FLAG-mLPCAT3-2ndPCR-R	CCGCTCGAGTCATTCCCTCTTTTTTAACTTTTCTTTTCTTGGC	1529
FLAG-mLPCAT4-2ndPCR-F	CTAGCTAGCCACCATGGATTACAAGGATGACGATGACAAGGCCACCACCAGCACCACGGGC	
FLAGmLPCAT4-2ndPCR-R	CCGCTCGAGTCACTGTGTTAGTGACGAGTGTCTGGAGCC	1621
FLAG-mLPEAT1-2ndPCR-F	CTAGCTAGCCACCATGGATTACAAGGATGACGATGACAAGGCAGCACGGCCGCCCGCCAGCC	
FLAG-mLPEAT1-2ndPCR-R	CCGCTCGAGTCAGTCTGCCTTCTTCTTTACAGAATTTGGACTCCG	1546
Primers for Quantitative RT-PCR		
mLPCAT3-QPCR-F	TCAGGATACCTGATTTGCTTCCA	
mLPCAT3-QPCR-R	GGATGGTCTGTTGCACCAAGTAG	151
mLPCAT4-QPCR-F	TTCGGTTTCAGAGGATACGACAA	
mLPCAT4-QPCR-R	AATGTCTGGATTGTCGGACTGAA	188
mLPEAT1-QPCR-F	CTGAAATGTGTGTGCTATGAGCG	
mLPEAT1-QPCR-R	TGGAAGAGAGGAAGTGGTGTCTG	178
mß-actin-QPCR-F	GCTGTGCTATGTTGCTCTAGACTT	
mß-actin-QPCR-R	AATTGAATGTAGTTTCATGGATGC	174

non-essential amino acids. P19 (pluripotent embryonal carcinoma) cells were grown in alpha MEM with 10% FBS. CHO-K1 (Chinese hamster ovary) cells were grown in Ham's F12 with 10% FBS.

Expression of mLPCAT3, mLPCAT4, and mLPEAT1 in CHO-K1 cells

After 48 h of transfection with vectors containing FLAG-tagged LPLAT cDNA using Lipofectamine 2000 (Invitrogen), cells from 10-cm dishes were scraped into 1 ml of ice-cold buffer containing 20 mM Tris-HCl (pH 7.4), 300 mM sucrose, and 1X Complete Protease Inhibitor (Roche Applied Science), and then sonicated for 30 s on ice three times. After centrifugation for 10 min at 800 x *g* (mLPCAT4 and mLPEAT1) or 9,000 x *g* (mLPCAT3), the supernatant was collected and centrifuged at 100,000 x *g* for 1 h. The resulting pellets were resuspended in buffer containing 20 mM Tris-HCl (pH 7.4), 300 mM sucrose, and 1 mM EDTA. Protein concentration was measured by the method of Bradford (37), using a commercially prepared protein assay solution (Bio-Rad) and bovine serum albumin (BSA, fraction V, fatty acid-free; Sigma) as a standard.

Western blot analysis

Microsomal protein (10 μg) was resolved by 10% SDS-PAGE and transferred to a Hybond ECL nitrocellulose membrane (Amersham Biosciences). The membrane was blocked with 5% skim milk, incubated with M2 anti-FLAG mouse monoclonal antibody (IBI/Kodak, Rochester, NY), washed, and then incubated with horseradish

peroxidase-linked anti-mouse IgG (Amersham Biosciences). After being washed, the membranes were exposed to ECL reagents (Amersham Biosciences) and x-ray film (Amersham Biosciences) to visualize immunoreactive proteins.

Immunofluorescence Microscopy

CHO-K1 cells were seeded onto 6-cm dishes before transfection. Then, 6 μg each of pCXN2.1 vector, or vector containing FLAG-mLPCAT3, -mLPCAT4 or -mLPEAT1 were transfected using Lipofectamine 2000 (Invitrogen). After transfection for 48 h, cells were fixed with 3.7% paraformaldehyde at 37°C for 30 min and washed three times with PBS. The fixed cells were permeabilized with methanol-acetone (1:1, v/v) at -20°C for 10 min, washed, and treated with 1% (w/v) BSA in PBS for 30 min at 37°C. After washing, cells were incubated with primary antibodies (10 μg/ml M5 anti-FLAG mouse monoclonal antibody or 5 μg/ml anti-FLAG rabbit polyclonal antibody; Sigma) at room temperature for 30 min, and washed. Next, cells were incubated with 10 μg/ml Alexa Fluor 546 goat anti-mouse IgG or alexa Fluor 488 goat anti-mouse IgG (Eugene, OR) at room temperature for 30 min. Anti-calnexin (Calbiochem), anti-GM130 (BD Biosciences), and anti-cytochrome c oxidase antibody (Invitrogen) were used as organelle markers for ER, Golgi apparatus and mitochondria, respectively.

Confocal microscopy was performed with an LSM510 laser-scanning microscope (Carl Zeiss) equipped with a 63x water immersion objective lens (numerical aperture = 1.2). Alexa Fluor 546 was monitored by excitation at 543 nm with a

helium/neon laser and by emission with a 585 nm long-pass filter. For the detection of Alexa Fluor 488, the cells were excited at 488 nm with an argon laser, and the emissions were collected with a 505–550-nm band pass filter.

Transmission electron microscopy (TEM)

For scanning TEM, empty vector or FLAG-tagged mLPCAT3 transfected CHO-K1 cells were treated with fixative containing 2% glutaraldehyde in 100 mM phosphate buffer. Electron micrographs were scanned by Filgen (Nagoya, Japan).

Isolation and Stimulation of Mouse Peritoneal Cells

Three days after intraperitoneal (i.p) injection of 2 ml of 4% thioglycolate, peritoneal exudate cells were harvested from the peritoneal cavity three times, each with 5 ml of ice-cold PBS. The cells were washed twice with 30 ml of ice-cold PBS after centrifugation at 250 x *g* at 4°C. Total cell numbers were determined with a hemocytometer after staining with Turk solution (Wako Pure Chemical Industries). Cells (3.2 x 10^6 cells/6-cm dish) were cultured in RPMI 1640 medium supplemented with 10% FBS (RPMI 1640–10% FBS) at 37°C in 5% CO_2. After incubation for 2 h, the medium was changed and the cells were further cultured in 4 ml of RPMI 1640–10% FBS for 20–22 h. The cells were treated with 100 ng/ml lipopolysaccharide (Sigma-Aldrich), 0.8 μM ODN1826, or 1 μg/ml poly(I:C) for 16 h. After treatment, the cells were washed with an ice-cold buffer containing 20 mM Tris-HCl (pH 7.4) and 300 mM sucrose, and used for quantitative RT-PCR analysis.

Quantitative Real Time RT-PCR

Mouse total RNA was prepared using the RNeasy Mini Kit (QIAGEN), and first strand cDNA was subsequently synthesized using Superscript II (Invitrogen). PCRs were performed using FastStart DNA Master SYBR Green I (Roche Applied Science) and a LightCycler 1.5 (Roche Applied Science). The primers for each enzyme are listed in Table 1.

In vitro LPLAT assays

The acyltransferase activity was measured in two ways: (i) by the transfer of [^{14}C]acyl-CoA to lysophospholipids to form phospholipids, and (ii) by conversion of [^{14}C]lysophospholipid to phospholipid in the presence of acyl-CoA. Reaction mixtures contained 100 mM Tris-HCl (pH 7.4), 0.5-1 mM EDTA, the indicated concentrations of acyl-CoA and lysophospholipid, and enzyme in a total volume of 0.1 ml. After incubation at 37°C for 10 min, reactions were stopped by the addition of 0.3 ml of chloroform:methanol (1:2, v/v). Total lipids were extracted using the Bligh-Dyer method (38), and subsequently analyzed by TLC in chloroform:methanol:acetic acid: water (50:25:8:4, v/v/v/v). Bands at positions corresponding to the expected products were visualized by I_2 vapor, excised from the plate, placed in Microscinti-O (PerkinElmer Life Sciences), and analyzed in a liquid scintillation counter LS6500 (Beckman).

siRNA Transfection

B16 cells were transfected with 50 nM mLPCAT3-siRNAs (mLPCAT3-siRNA#1, ID number 89055; #2, 89150; #3, 89240), mLPCAT4-siRNAs (mLPCAT4-siRNA#1, 79688; #2, 79779; #3, 179488), mLPEAT1-siRNAs (mLPEAT1-siRNA#1, 93126; #2, 93219; #3, 170568), or NC-siRNA (silencer negative control 1) for 2-4 days, using Lipofectamine 2000, according to the manufacturer's protocol. siRNA were obtained from Ambion.

Analysis of phospholipids using electrospray ionization mass spectrometry (ESI-MS)

Forty-eight hours after transfection, cells were supplemented with 10 nM arachidonic acid for 24 h, and then total lipids were extracted by the Bligh-Dyer method (38); PBS:chloroform:methanol (1:1.25:2.5 ml), chloroform (1.25 ml), and water (1.25 ml) were used as extraction solvents. The ESI-MS/MS analysis was performed using a 4000 Q-TRAP quadrupole linear ion trap hybrid mass spectrometer (Applied Biosystems/MDS Sciex, Concord, ON, Canada) with an ACQUITY Ultra Performance LC® (Waters, Milford, MA). Each sample was injected onto an ACQUITY UPLC™ BEH C18 column (1.0 mm x 150 mm i.d., 1.7 μm particle) and then subjected directly to ESI-MS/MS analysis. Five microliters of sample were directly introduced by autosampler injection, and the samples were separated by a step gradient with mobile phase A (acetonitrile:methanol:water [2:2:1 v/v/v], containing 0.1% formic acid and 0.028% ammonium) and mobile phase B (isopropanol containing 0.1% formic acid and 0.028% ammonium) at the following ratios: 100:0 (0–5 min), 95:5 (5–20 min), and

70:30 (20–21 min). Subsequently, the concentration of mobile phase B was increased to 50% by a linear gradient for 24 min (21-45 min), and was retained at 50% of mobile phase B (50:50) for 45 min (45-90 min), and then at 0% of mobile phase B (100:0) for 30 min (90-120). The reaction was performed at a flow rate of 70 μl/min and the column temperature was maintained at 30°C. The method to identify phospholipid species was described previously (39).

Mice

C57BL/6J mice were obtained from Clea Japan, Inc. (Tokyo, Japan). All animal studies were conducted in accordance with the guidelines for Animal Research at The University of Tokyo, and were approved by the University of Tokyo Ethics Committee for Animal Experiments.

Results

Cloning of mouse LPCAT3, LPCAT4, and LPEAT1

To identify novel LPLATs, I focused on uncharacterized proteins in the MBOAT family. A phylogenetic tree was drawn by pairwise comparisons of amino acid sequences of AGPAT, diacylglycerol AT2 (DGAT2), and MBOAT family members using ClustalW, European Bioinformatics Institute (EBI) (http://www.ebi.ac.uk/) (40) (Fig. 3A). The cluster of MBOAT family proteins comprising new LPLATs was different from that of the AGPAT or DGAT2 family. Mouse MBOAT5, 2, and 1 were designated as mLPCAT3, mLPCAT4, and mLPEAT1, respectively, based on their activities characterized in this study (see below). The functionally identified LPLATs are summarized in Figure 3B, with the higher enzymatic activities for acyl-CoAs are indicated. The putative open reading frames of mLPEAT1, mLPCAT4, and mLPCAT3 encoded proteins of 492 amino acids (aa) (56.1 kDa), 519 aa (58.9 kDa), and 487 aa (56.1 kDa), respectively (Fig. 4), and these proteins. Boxes indicate that mLPCAT3, mLPCAT4, and mLPEAT1 were predicted by HMMTOP (41) to possess 10, 4, and 9 putative transmembrane domains, respectively. While the enzyme sequences did not reveal AGPAT motifs as described above, LPCAT3 and LPEAT1 were found to possess the C-terminal sequence motif KKXX (33), suggesting that these proteins are localized to the ER in the same way as LPCAT1 and LPCAT2 are (30,31).

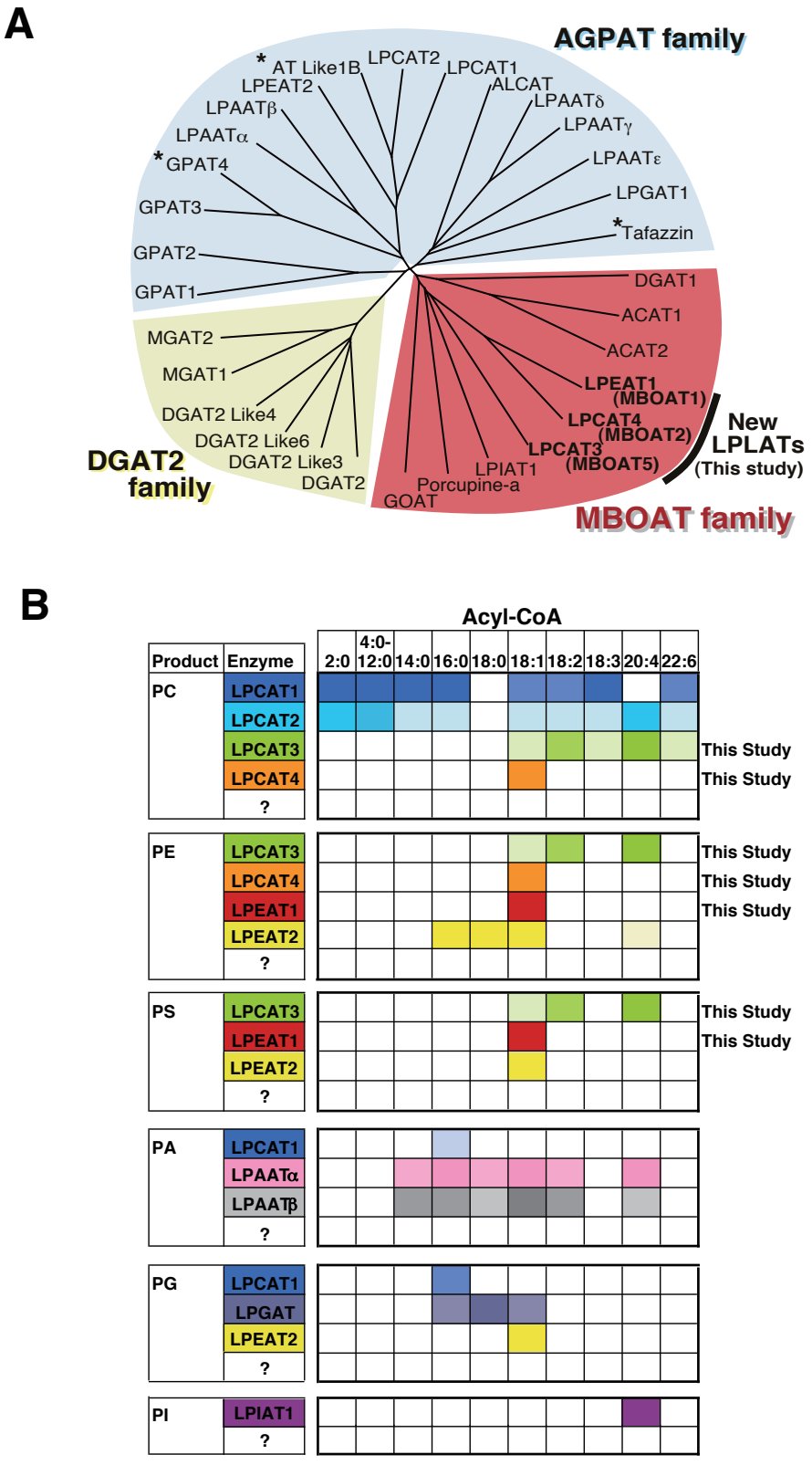

Fig. 3. Phylogenetic tree of mouse LPLAT family and summary of characterized LPLATs.
(A) A phylogenetic tree was drawn using ClustalW (http://www.ebi.ac.uk/). Values show branch lengths that represent the evolutional distance between each pair of sequences. Putative LPLAT genes are indicated by asterisks (*). Sequence data of mouse acyltransferases are available in the DDBJ/EMBL/GenBank databases. The accession numbers are shown in Table 2. (B) Functionally identified LPLATs were summarized. The darker color indicates higher enzymatic activity for acyl-CoAs. Novel enzymes, LPCAT3, LPCAT4, and LPEAT1 are shown in "This study" . Additional LPLATs that may exist were shown in "?" . GPAT, glycerol-3-phosphate acyltransferase; MGAT, monoacylglycerol O-acyltransferase; ACAT, sterol O-acyltransferase; GOAT, Ghrelin O-acyltransferase.

Table 2

Family	Acyltransferase	Accession No.
LPAAT	GPAT1	NP_032175
	GPAT2	XP_130488
	GPAT3	NP_766303
	GPAT4	NP_997089
	LPAATα	NP_061350
	LPAATβ	NP_080488
	LPAATγ	NP_443747
	LPAATδ	NP_080920
	LPAATε	NP_081068
	LPEAT	NP_061213
	AT Like 1B	NP_081875
	LPGAT1	NP_758470
	ALCAT	Q3UN02
	LPCAT1	BAE94687
	LysoPAFAT/LPCAT2	BAF47695
	Tafazzin	NP_852657
DGAT2	MGAT1	NP_080989
	MGAT2	NP_803231
	DGAT2	NP_080660
	DGAT2Like3	NP_001074605
	DGAT2Like4	NP_808414
	DGAT2Like6	CAM19588
MBOAT	LPCAT3 (MBOAT5)	NP_660112
	LPCAT4 (MBOAT2)	NP_080313
	LPEAT1 (MBOAT1)	NP_705774
	GOAT1	XP_134120
	DGAT1	NP_034176
	ACAT1	NP_033256
	ACAT2	NP_666176
	Porcupine-a	NP_058609
	LPIAT1	NP_084210

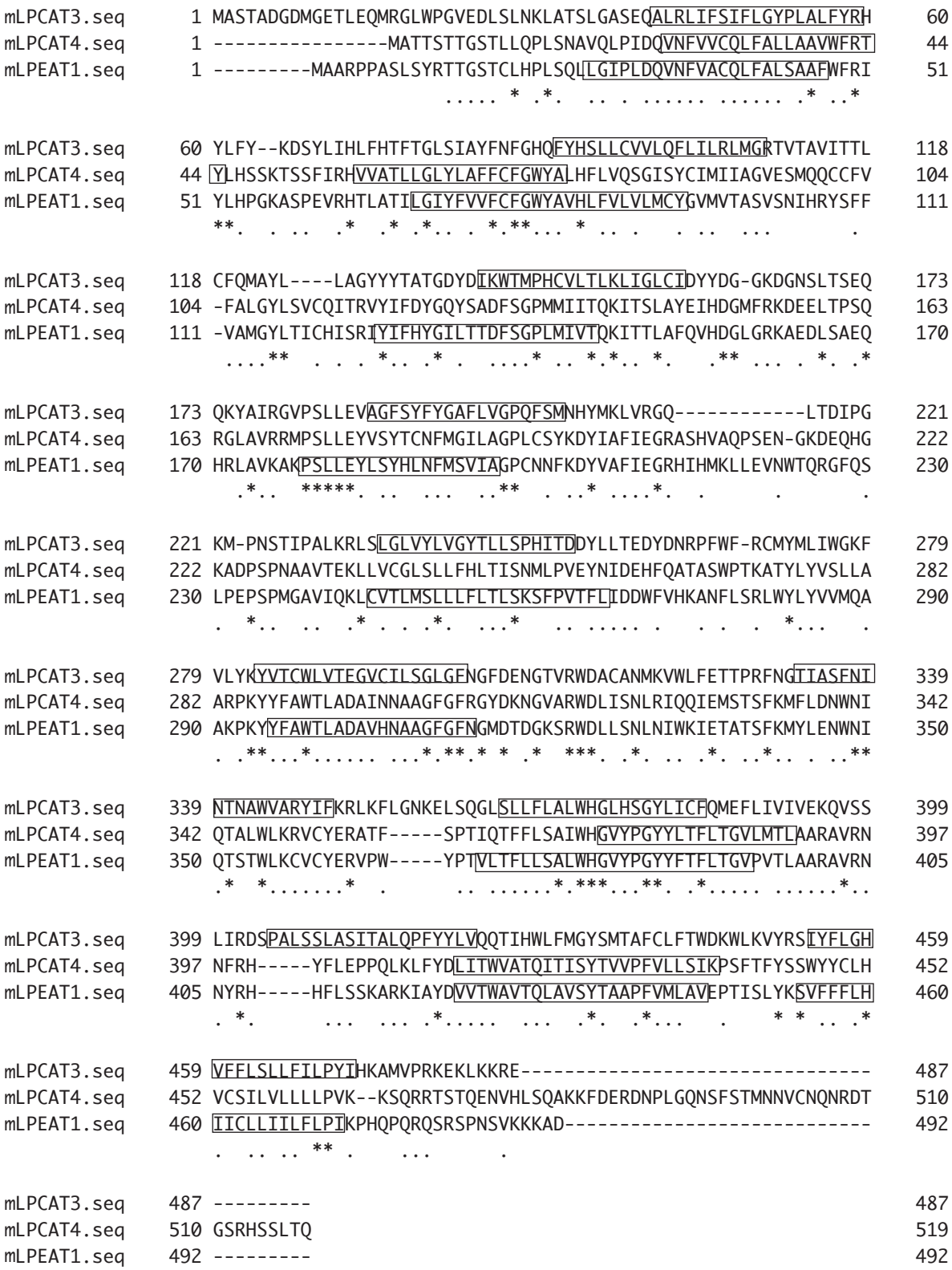

Fig. 4. Amino acid sequence alignments of mLPCAT3, mLPCAT4, and mLPEAT1.
Amino acids conserved among the enzymes are marked with asterisks (*). The ER localization sequence KKXX is present at the C terminus of mLPCAT3 and mLPEAT1. The putative transmembrane motifs were determined using HMMTOP (http://www.enzim.hu/hmmtop/index.html) and boxed.

Subcellular localization of mLPCAT3, mLPCAT4, and mLPEAT1

To facilitate Western blot and immunocytochemical analyses of mLPCAT3, mLPCAT4, and mLPEAT1, plasmids expressing N-terminal FLAG-tagged recombinant enzymes were constructed. Microsomal proteins (100,000 x *g*, 1 h pellet) of CHO-K1 cells transfected with empty vector or with vector containing FLAG-tagged cDNA corresponding to each enzyme were subjected to Western blot analysis, which revealed apparent molecular weights of 40 kDa, 42 kDa, and 40 kDa for mLPCAT3, mLPCAT4 and mLPEAT1, respectively (Fig. 5A). These results are inconsistent with the molecular weights calculated from the deduced amino acid sequences (i.e. 56.1 kDa, 58.9 kDa, and 56.1 kDa, respectively), which could be due to the numerous predicted membrane-spanning structures predicted to occur these proteins (Fig. 4) affecting their mobility during SDS-PAGE. The subcellular localization of these enzymes was examined by confocal microscopy. mLPCAT3, mLPCAT4, and mLPEAT1 co-localized with calnexin, an ER marker protein, suggesting that these enzymes are present mainly in the ER (Fig. 5B). Neither Golgi marker protein (GM130) nor mitochondrial marker protein (cytochrome *c* oxidase) colocalized with the enzymes (Fig. 6A and B). The distribution patterns of the enzymes were confirmed by cell fractionation and Western blotting (Fig. 6C). Importantly, overexpression of these enzymes in CHO cells produced unidentified organelles (Fig. 5B, arrowheads). Surprisingly, the staining pattern of the unidentified organelles co-localized with each enzyme and also with calnexin (Fig. 5B, arrowheads). To investigate these organelles, I analyzed CHO-K1 cells transfected with mLPCAT3 by transmission electron microscopy. Although the ER structure was the

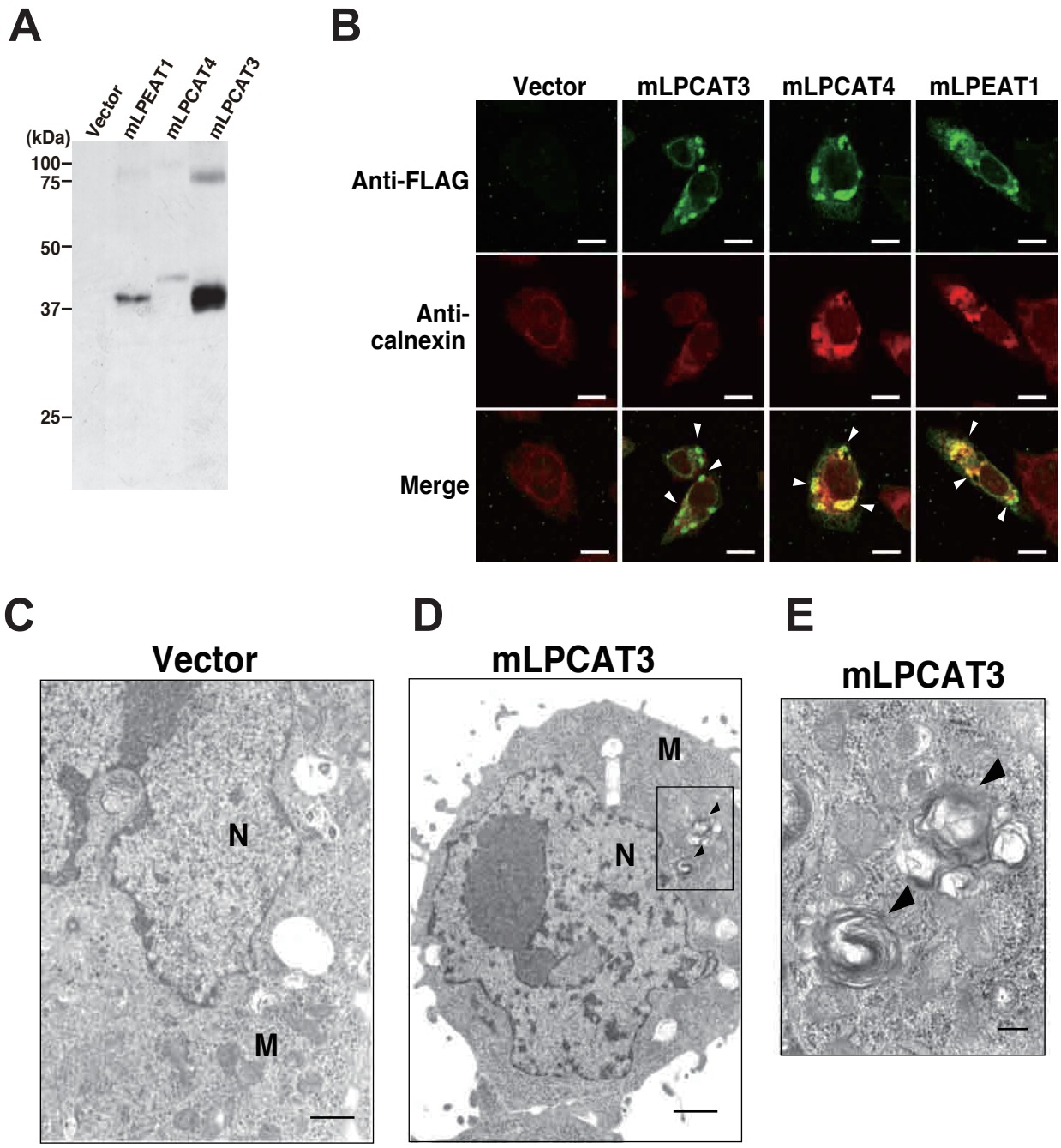

Fig. 5. Western blot analysis and subcellular localization of FLAG-tagged mLPCAT3, mLPCAT4, and mLPEAT1, and transmission electron microscopy (TEM) of mLPCAT3 in CHO-K1 cells.

After 48 h of transfection, CHO-K1 cells were subjected to following analyses. (A) An amount of 10 μg protein of the 100,000 x *g* pellet fraction from transfected CHO-K1 cells was analyzed by Western blot using M2 anti-FLAG antibody. Molecular sizes were indicated on the left in kDa. Results were representative of three independent experiments. (B) ER and FLAG-tagged enzymes were visualized using an anti-calnexin antibody (red) and an anti-FLAG antibody (green), respectively. The subcellular localizations of all enzymes were similar to the ER marker (merge staining patterns, yellow). The scale bars correspond to 20 μm. Two independent experiments were performed with similar results. Arrowheads indicated karmellae-like membrane structures. (C-E) CHO-K1 cells transiently transfected with (C) vector or (D and E) FLAG-tagged mLPCAT3 cDNA were imaged by TEM. (E) The boxed area in panel C was magnified. M, mitochondria; N, nucleus. The arrowheads indicated the multilayer membrane components (karmellae like structures). The scale bars corresponded to (C and D) 1 μm, and (E) 100 nm. Two independent experiments were performed with similar results.

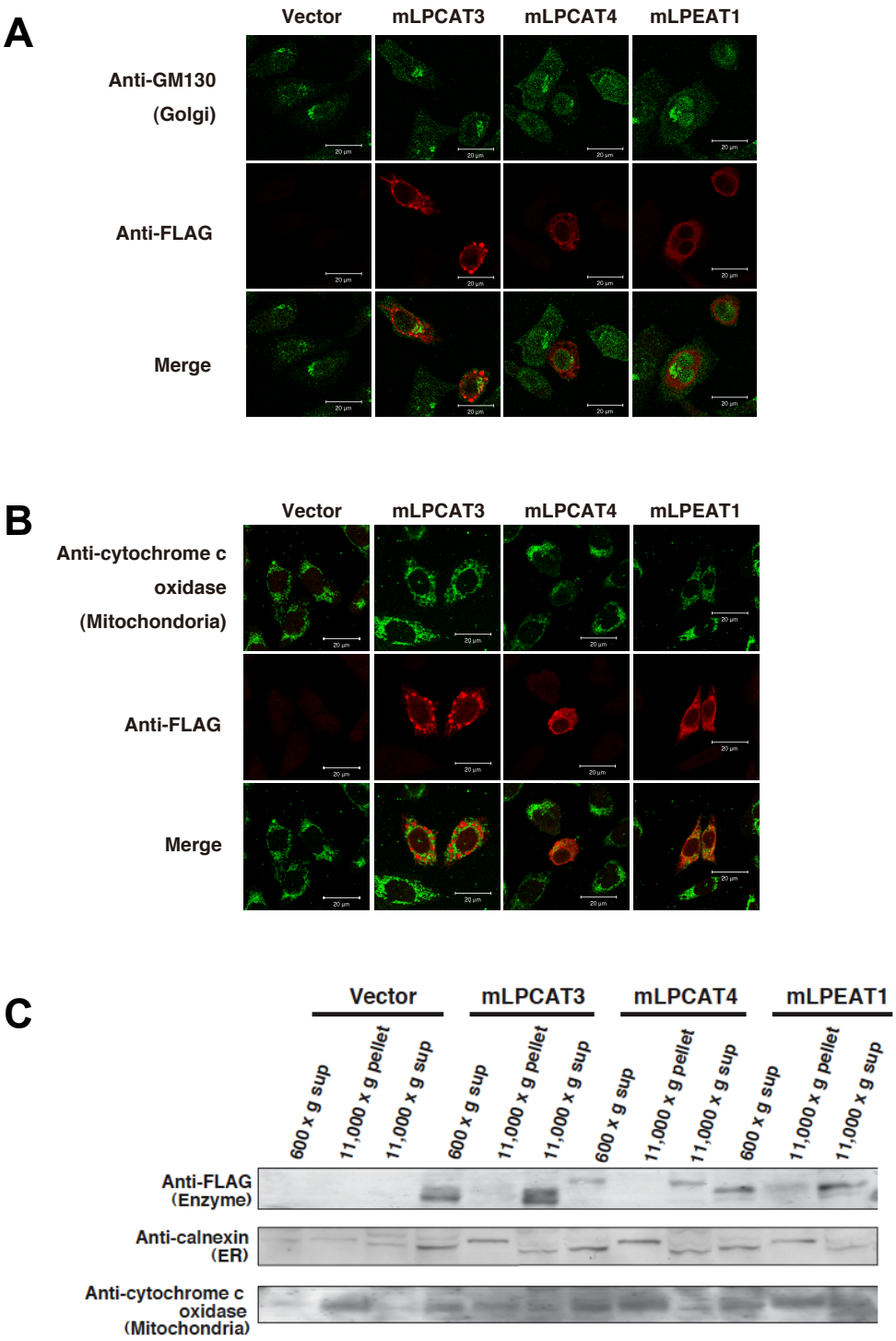

Fig. 6. Western blot analysis and immunocytochemistry of FLAG-tagged mLPCAT3, mLPCAT4, and mLPEAT1.

After 48 h of transfection, CHO-K1 cells were subjected to immunocytochemical and Western blot analysis. (A and B) Golgi (A), mitochondria (B), and FLAG-tagged enzymes were visualized using an anti-GM130 antibody (green), anti-cytochrome c oxidase antibody (green), and anti-FLAG antibody (red), respectively. The subcellular localization of all enzymes was not merged with Golgi and mitochondria marker proteins. The scale bars correspond to 20 μm. Two independent experiments were performed with similar results. (C) The mitochondrial fraction was isolated from transfected CHO-K1 cells using Cell Mitochondria Isolation Kit (Sigma). We obtained the three fractions: (i) whole cell lysate (600 x *g* supernatant); (ii) mitochondria fraction (11,000 x *g* pellet); and (iii) 11,000 x *g* supernatant including the ER fraction. The equal volumes of obtained fractions were subjected to Western blot analyses using anti-FLAG antibody, anti-calnexin antibody, or anti-cytochrome c oxidase antibody. FLAG-tagged enzymes were detected mainly in the 11,000 x *g* supernatant. Two independent experiments were performed with similar results.

same in CHO-mLPCAT3 and CHO-Vector cells, atypical multilayer membrane components (karmellae-like structures) (42) were observed (Fig. 5D and E). The number and size of these structures were greater in CHO-mLPCAT3 cells than in CHO-Vector cells (Fig. 5C-E). The nature and origin of these structures remain to be clarified.

Tissue distribution of mLPCAT3, mLPCAT4, and mLPEAT1

Tissue distribution of mLPCAT3, mLPCAT4, and mLPEAT1 was analyzed using quantitative real-time RT-PCR analyses. The mRNA of mLPCAT3 was detected ubiquitously with high expression levels in the testis (Fig. 7A). In contrast, mLPCAT4 mRNA was highly expressed in the epididymis, brain, testis, and ovary; and mLPEAT1 mRNA in the stomach, epididymis, and colon (Fig. 7B and C). mRNA levels of ß-actin were used to normalize the mRNA levels of each enzyme.

Effect of an inflammatory stimulus on the mRNA expression of mLPCAT3, mLPCAT4, and mLPEAT1

Several studies have described a possible relationship between LPLAT activities and inflammatory responses (43-45). Indeed, Up-regulation of LPCAT2 mRNA by the stimulation with toll-like receptors (TLR4 and 9) agonist was reported in mouse macrophages (31). Thus, to characterize the new LPLATs, I investigated the effect of an inflammatory stimulation on the expression of their mRNA expression. Mouse macrophages were treated with lipopolysaccharide (TLR4 agonist), ODN1826

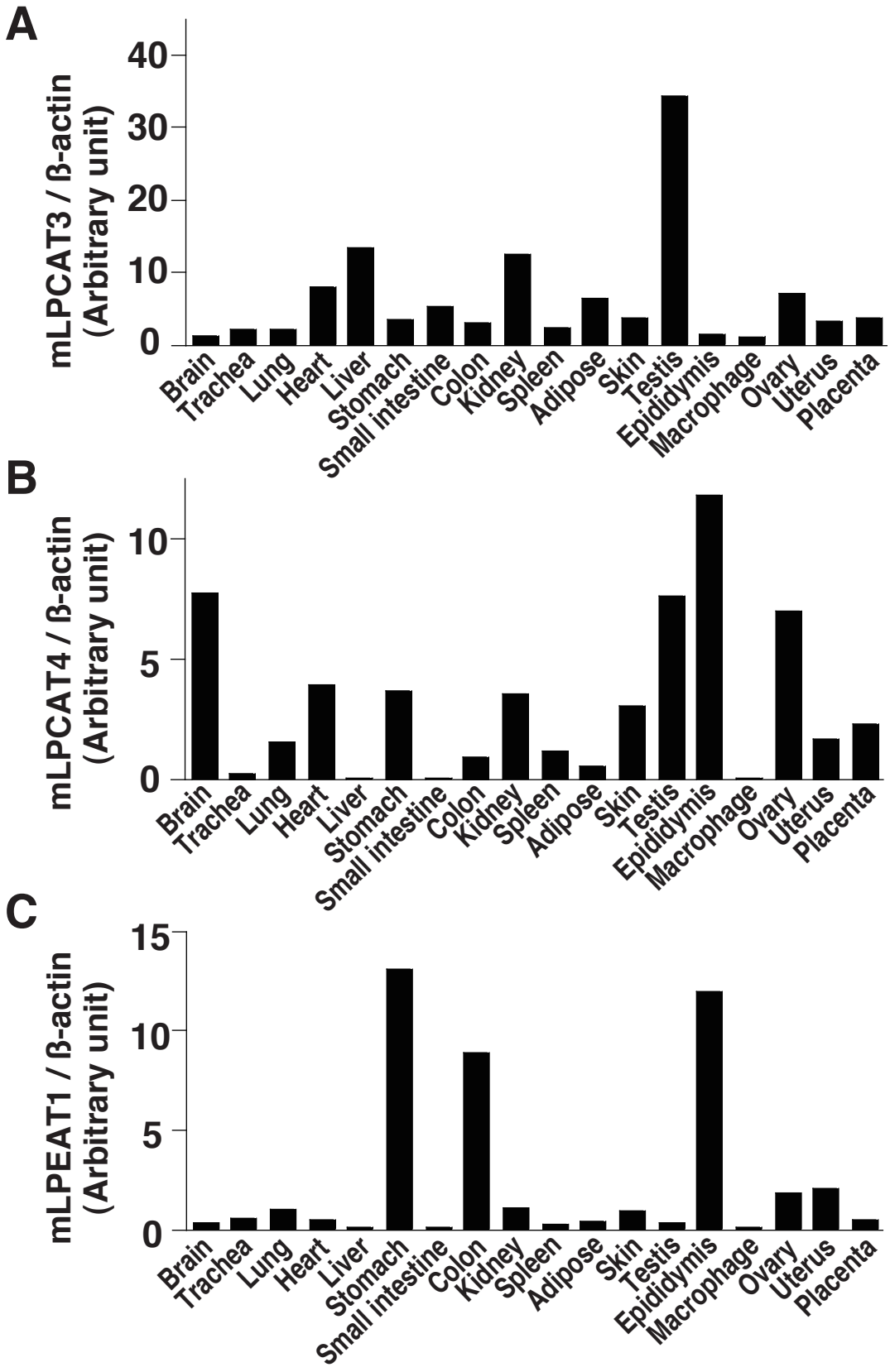

Fig. 7. Tissue distribution of mLPCAT3, mLPCAT4, and mLPEAT1 mRNA expression. The expression levels of (A) mLPCAT3, (B) mLPCAT4, (C) mLPEAT1 in 18 mouse tissues were analyzed by quantitative RT-PCR. The levels of these mRNAs were normalized using ß-actin levels. Two independent experiments were performed with similar results.

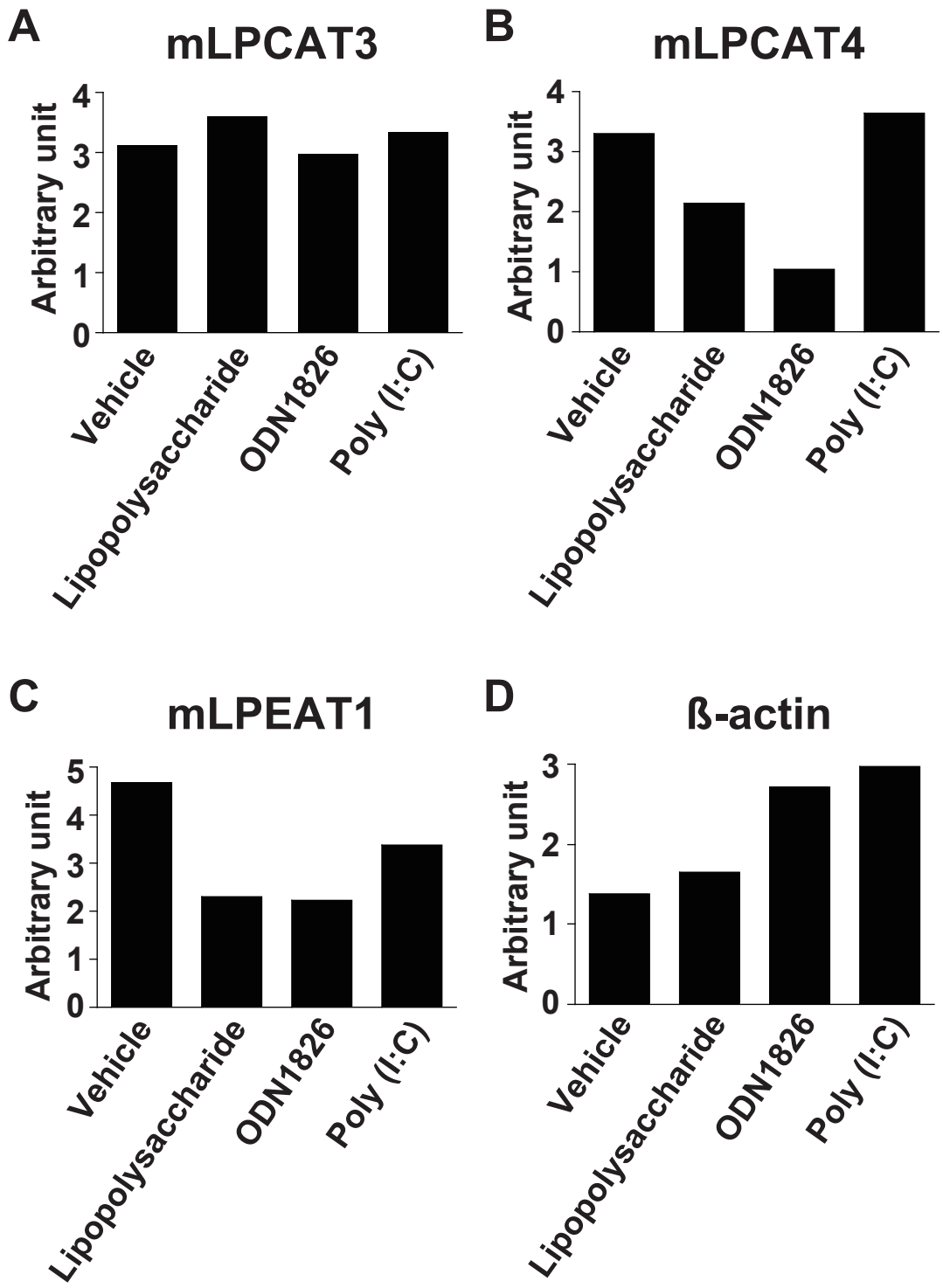

Fig. 8. Effect of an inflammatory stimulus on the mRNA expression of mLPCAT3, mLPCAT4, and mLPEAT1.

Mouse peritoneal macrophages were stimulated by 100 ng/ml Lipopolysaccharide, 0.8 μM ODN1826, or 1 μg/ml poly(I:C) for 16 h. The levels of (A) mLPCAT3, (B) mLPCAT4, (C) mLPEAT1, and (D) ß-actin mRNA were analyzed by quantitative RT-PCR.

(TLR9 agonist), and Poly(I:C) (TLR3 agonist) for 16 h. However, treatment with these TLR agonists did not affect the expression levels of mLPCAT3, mLPCAT4, or mLPEAT1 (Fig. 8).

LPLAT activities of FLAG-tagged mLPCAT3, mLPCAT4, and mLPEAT1

I next examined the LPLAT activities of FLAG-tagged mLPCAT3, using a variety of lysophospholipids as acceptors and acyl-CoAs as donors. mLPCAT3 exhibited detectable LPLAT activity for LPC, LPE, and LPS when arachidonoyl-CoA was used (Fig. 9A). In contrast, mLPCAT4 possessed LPCAT and LPEAT activities (Fig. 10A), and mLPEAT1 showed LPEAT and LPSAT activities when oleoyl-CoA was used (Fig. 11A). mLPCAT3 recognized various polyunsaturated fatty acyl-CoAs, while mLPCAT4 and mLPEAT1 demonstrated preferential activity for oleoyl-CoA (Fig. 9B, D, F; Fig. 10B and D; Fig. 11B and D; Table 3).

mLPCAT3 and mLPCAT4 exhibited enzymatic activity for various acyl groups at the *sn*-1 position of LPC; a higher activity was observed for when 1-acyl-LPC was used as an acceptor than when 1-*O*-alkyl-LPC or 1-*O*-alkenyl-LPC was used (Fig. 9C and Fig. 10C). There were no clear differences in the activities of mLPCAT3, mLPCAT4, and mLPEAT1 for 1-acyl-LPEAT and 1-*O*-alkenyl-LPEAT (Fig. 9E, Fig.10E, and Fig. 11C). mLPCAT3 and mLPEAT1 showed higher activity for 1-oleoyl-LPE than 1-palmitoyl-LPE (Fig. 11C, and Fig. 9E), while mLPCAT4 showed a preference for 1-palmitoyl-LPE (Fig. 10E). Furthermore, mLPCAT3 and mLPEAT1 recognized both 1-oleoyl-LPS and a crude mixture of LPS (Fig. 9G and Fig. 11E). The

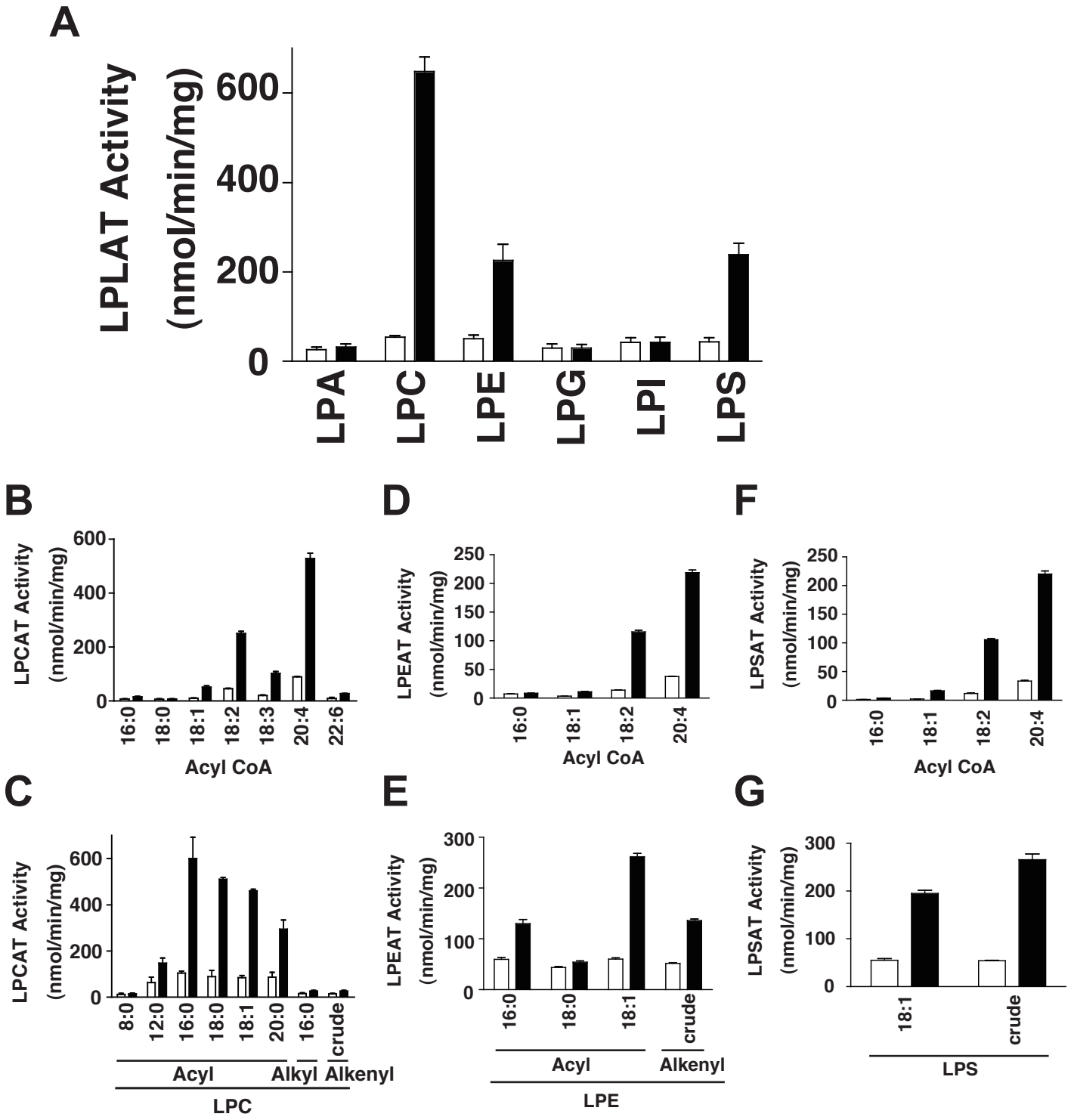

Fig. 9. Substrate selectivity of mLPCAT3.

LPLAT assays were performed by TLC with several 50 μM lysophospholipids and 25 μM acyl-CoAs using 0.5 μg of microsomal proteins from vector-transfected (open bars) or mLPCAT3-transfected (closed bars) CHO-K1 cells. (A) The LPLAT activities of mLPCAT3 were measured using several lysophospholipids and [^{14}C]arachidonoyl-CoA. (B and C) LPCAT activities of mLPCAT3 using (B) acyl-CoA (16:0, 18:0, 18:1, 18:2, 18:3, 20:4, and 22:6) with [^{14}C]LPC (C16:0) or (C) several LPC (1-acyl LPC C8:0, 12:0, 16:0, 18:0, 18:1, 20:0, 1-alkyl LPC C16:0 and crude 1-alkenyl LPC) with [^{14}C]arachidonoyl-CoA were measured. (D-F) LPEAT and LPSAT activities of mLPCAT3 using; [^{14}C]acyl-CoA (16:0, 18:1, 18:2, and 20:4) with (D) LPE (C18:1) or (F) LPS (C18:1); or using [^{14}C]arachidonoyl-CoA with (E) LPE (1-acyl LPE C16:0, 18:0, 18:1, and crude 1-alkenyl LPE) or (G) LPS (1-acyl LPS C18:1 and crude 1-acyl LPS) were measured. The data represent the mean + S.D. of triplicate measurements. Two independent experiments were performed with similar results.

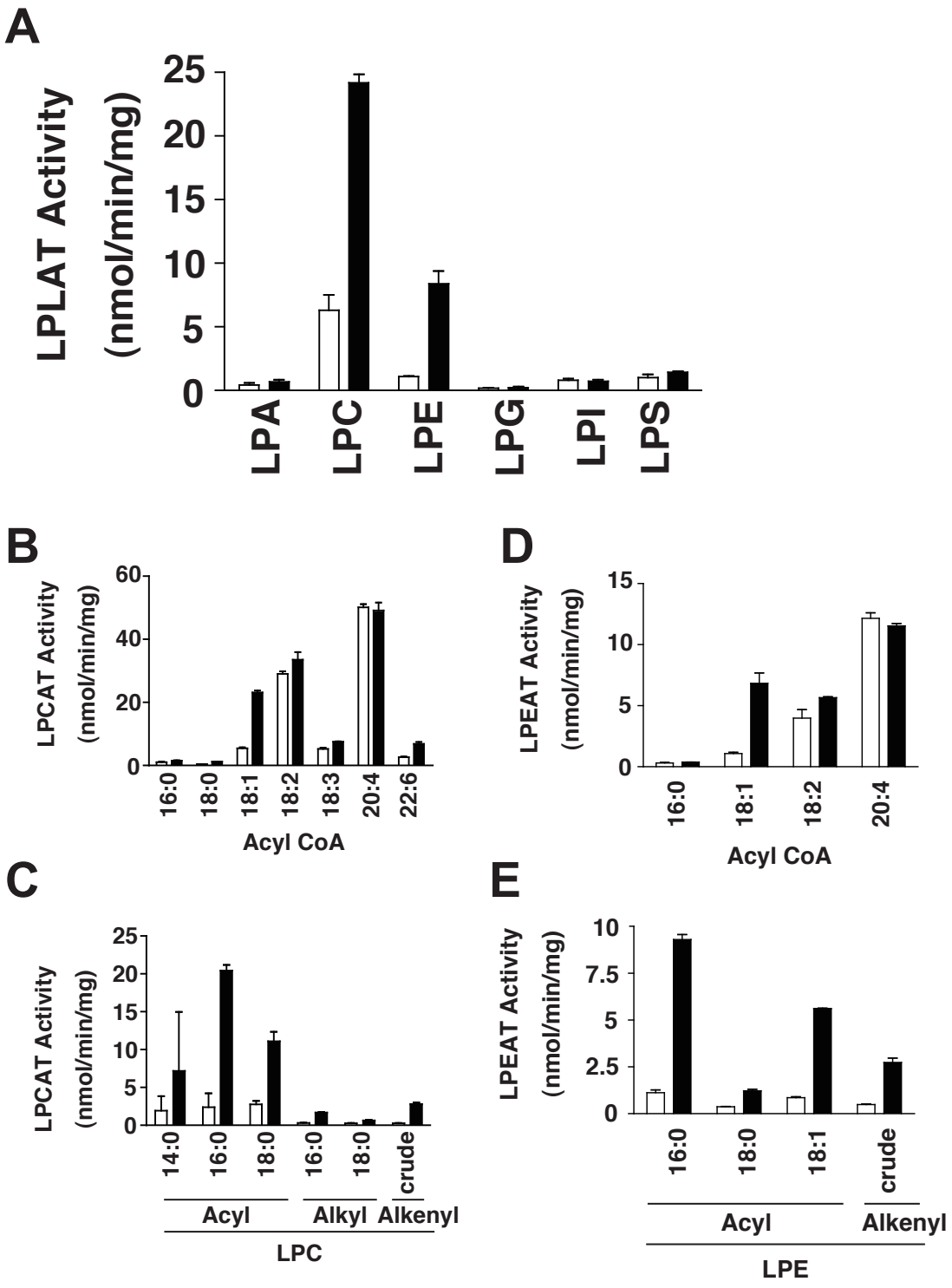

Fig. 10. Substrate selectivity of mLPCAT4.

LPLAT assays were performed by TLC with several 100 μM lysophospholipids and 50 μM acyl-CoAs using 5 μg of microsomal proteins from vector-transfected (open bars) or mLPCAT4-transfected (closed bars) CHO-K1 cells. (A) The LPLAT activities of mLPCAT4 were measured using several lysophospholipids and [^{14}C]oleoyl-CoA. (B and C) LPCAT activities of mLPCAT4 using (B) acyl-CoA (16:0, 18:0, 18:1, 18:2, 18:3, 20:4, and 22:6) with [^{14}C]LPC (C16:0) or (C) several LPC (1-acyl LPC C8:0, 12:0, 16:0, 18:0, 18:1, 20:0, 1-alkyl LPC C16:0 and crude 1-alkenyl LPC) with [^{14}C]oleoyl-CoA were measured. (D and E) LPEAT activities of mLPCAT4 were measured using (D) [^{14}C]acyl-CoA (16:0, 18:1, 18:2, and 20:4) with LPE (C16:0) or (E) [^{14}C]oleoyl-CoA with LPE (1-acyl LPE C16:0, 18:0, 18:1, and crude 1-alkenyl LPE). The data represent the mean + S.D. of triplicate measurements. Two independent experiments were performed with similar results.

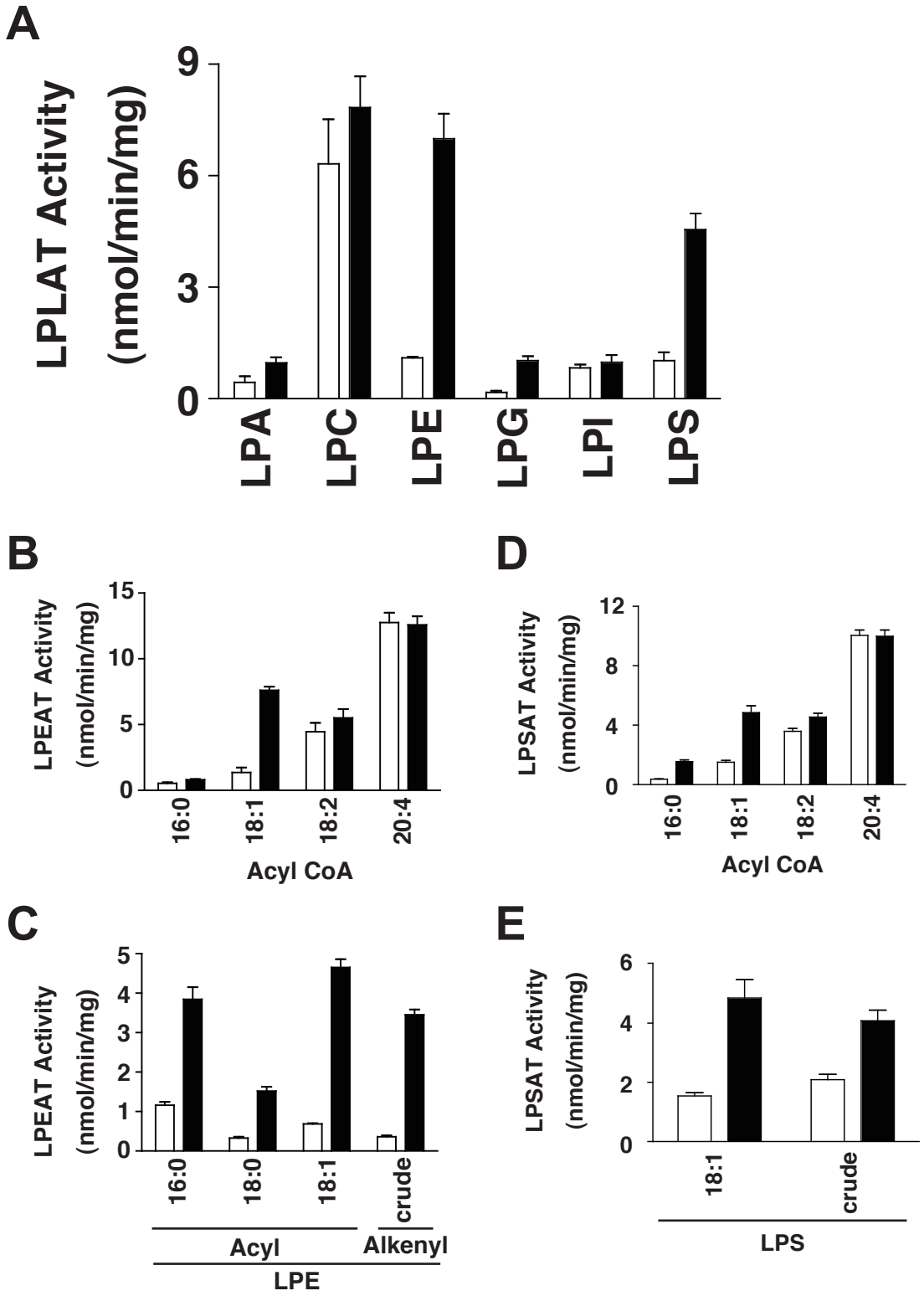

Fig. 11. Substrate selectivity of mLPEAT1.

LPLAT assays were performed by TLC with several 100 μM lysophospholipids and 50 μM acyl-CoAs using 5 μg of microsomal proteins from vector-transfected (open bars) or mLPEAT1-transfected (closed bars) CHO-K1 cells. (A) The LPLAT activities of mLPEAT1 were measured using several lysophospholipids and [^{14}C]oleoyl-CoA. (B and C) LPEAT activities of mLPEAT1 were measured using (B) [^{14}C]acyl-CoA (16:0, 18:1, 18:2, and 20:4) with LPE (C16:0) or (C) [^{14}C]oleoyl-CoA with LPE (1-acyl LPE C16:0, 18:0, 18:1, and crude 1-alkenyl LPE). (D and E) LPSAT activities of mLPEAT1 were using (D) [^{14}C]acyl-CoA (16:0, 18:1, 18:2, and 20:4) with LPS (C18:1) or (E) [^{14}C]oleoyl-CoA with LPS (1-acyl LPS C18:1 and crude 1-acyl LPS) were measured. The data represent the mean + S.D. of triplicate measurements. Two independent experiments were performed with similar results.

Table 3

Substrate selectivities of three acyltransferases

Enzyme	Enzymatic Activity	AcylCoA	Lysophospholipid
mLPCAT3	LPCAT	20:4 > 18:2 > 18:3 > 18:1 > 22:6	16:0 > 18:0 > 18:1 > 20:0 > 12:0
	LPEAT	20:4 > 18:2 > 18:1	18:1 > 16:0 = alkenyl (crude)
	LPSAT	20:4 > 18:2 > 18:1	18:1
mLPCAT4	LPCAT	18:1	16:0 > 18:0
	LPEAT	18:1	16:0 > 18:1 > alkenyl (crude) > 18:0
mLPEAT1	LPEAT	18:1	18:1 > 16:0 > alkenyl (crude) > 18:0
	LPSAT	18:1	18:1

Table 4

The *K*m and *V*max values of three acyltransferases for each substrate

			AcylCoA			Lysophospholipid		
Enzyme	Enzymatic Activity	Substrate	*K*m (μM)	*V*max (nmol/min/mg)	*K*m / *V*max	*K*m (μM)	*V*max (nmol/min/mg)	*K*m / *V*max
mLPCAT3	LPCAT	16:0LPC / 20:4CoA	6.1-9.5	914-978	102.9-149.9	33.8-35.2	1098-1352	32.5-38.4
	LPEAT	18:1LPE / 20:4CoA	43.2-45	475-491	10.9-11.0	27.5-31.9	273-318	9.9-10.0
	LPSAT	18:1LPS / 20:4CoA	23.2-32.8	275-318	9.7-11.9	17.0-27.6	350-400	14.5-20.6
mLPCAT4	LPCAT	16:0LPC / 18:1CoA	4.1-6.5	17.8-30.0	4.3-4.6	6.9-8.9	20.8-28.4	3.0-3.2
	LPEAT	16:0LPE / 18:1CoA	47.3-49.0	32.5-42.8	0.7-0.9	17.5-37.9	9.7-20.2	0.5-0.5
mLPEAT1	LPEAT	18:1LPE / 18:1CoA	3.3-6.1	8.7-13.1	2.1-2.6	7.2-8.3	6.6-8.1	0.9-1.0
	LPSAT	18:1LPS / 18:1CoA	3.2-4.6	3.4-5.1	0.7-1.6	1.8-2.7	4.5-5.8	2.1-2.5

substrate selectivity and the apparent *K*m and *V*max values of the enzymes are summarized in Table 3 and Table 4, respectively. mLPCAT3 showed higher LPCAT activity than LPEAT and LPSAT activities (Fig. 9A). Similarly, mLPCAT4 had higher LPCAT activity than LPEAT activity (Fig. 10A). mLPEAT1 showed similar activities for LPE and LPS (Fig. 11A and Table 4). The specific activities of mLPCAT3 were much higher than those of mLPCAT4 or mLPEAT1, partly because protein expression level of mLPCAT3 was extremely high (see Fig. 5A).

Reduction of endogenous LPLAT activities by mLPCAT3 siRNA

I next investigated the role of endogenous mLPCAT3. I selected to perform siRNA transfection in B16 melanoma cells, because these cells exhibit high levels of mRNA expression of mLPCAT3, mLPCAT4, and LPEAT1 mRNA in 18 different mouse-derived cell lines (Fig. 12). To investigate whether endogenous LPLAT activities are decreased by mLPCAT3-, mLPCAT4, and mLPEAT1-siRNA, I transfected B16 cells with siRNAs designed against three different regions of these new LPLAT genes or with a negative control (NC)-siRNA. Each siRNA decreased the mRNA expression of the target gene by 20-30% relative to NC-siRNA without affecting the mRNA expression of other two LPLATs I identified in this study (Fig. 13).

Endogenous LPCAT, LPEAT, and LPSAT activities, measured using arachidonoyl-CoA as a donor, were shown to decrease in cells transfected with mLPCAT3-siRNA (Fig. 14A). In cells transfected with siRNAs against mLPCAT4 and mLPEAT1, endogenous LPLAT activities for oleoyl-CoA remained unchanged (Fig.

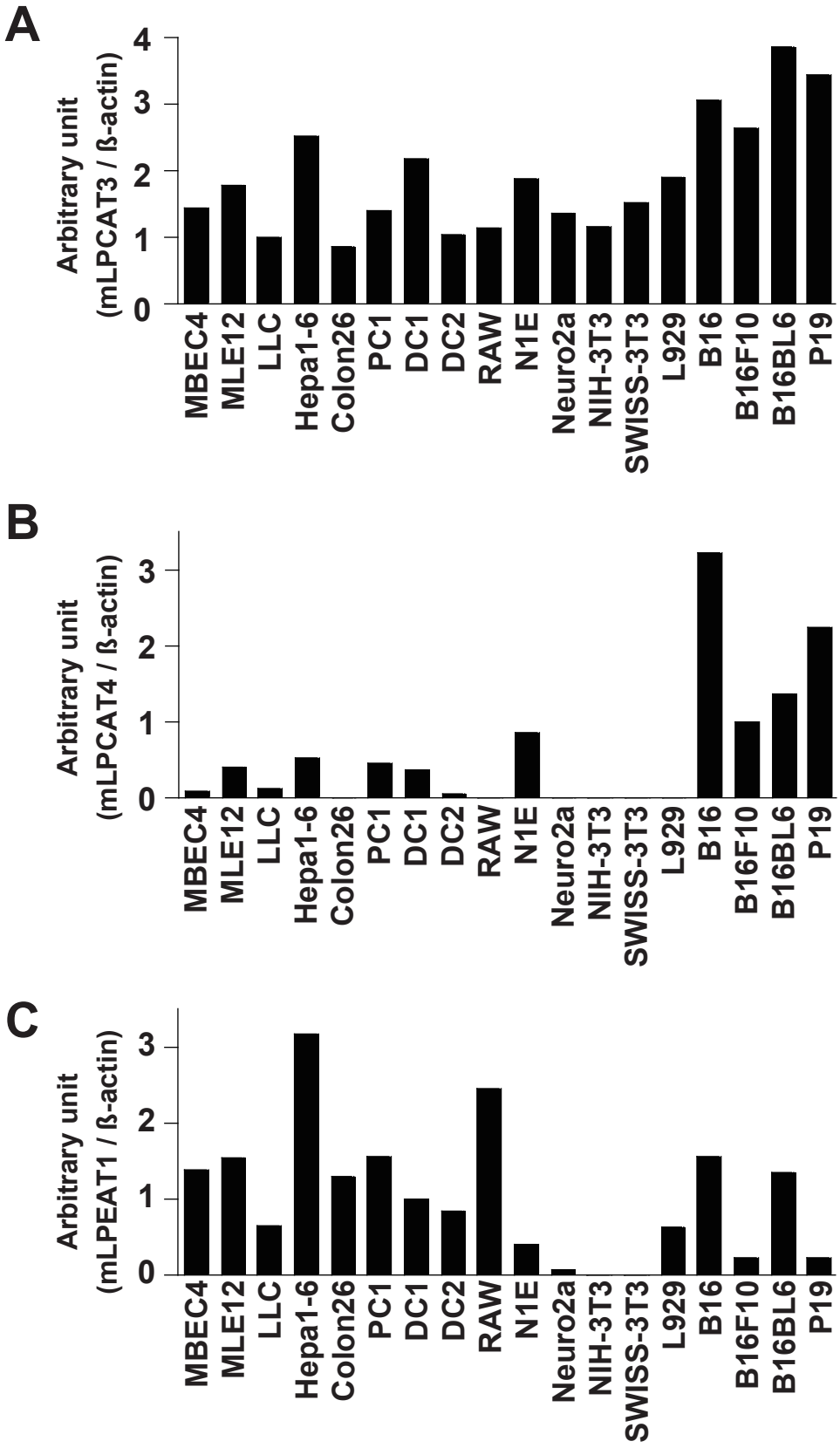

Fig. 12. The mRNA expression of mLPCAT3, mLPCAT4, and mLPEAT1 in various mouse-derived cell lines.

The expression levels of (A) mLPCAT3, (B) mLPCAT4, (C) mLPEAT1 in 18 different mouse-derived cell lines were analyzed by quantitative RT-PCR. The levels of these mRNAs were normalized using ß-actin levels.

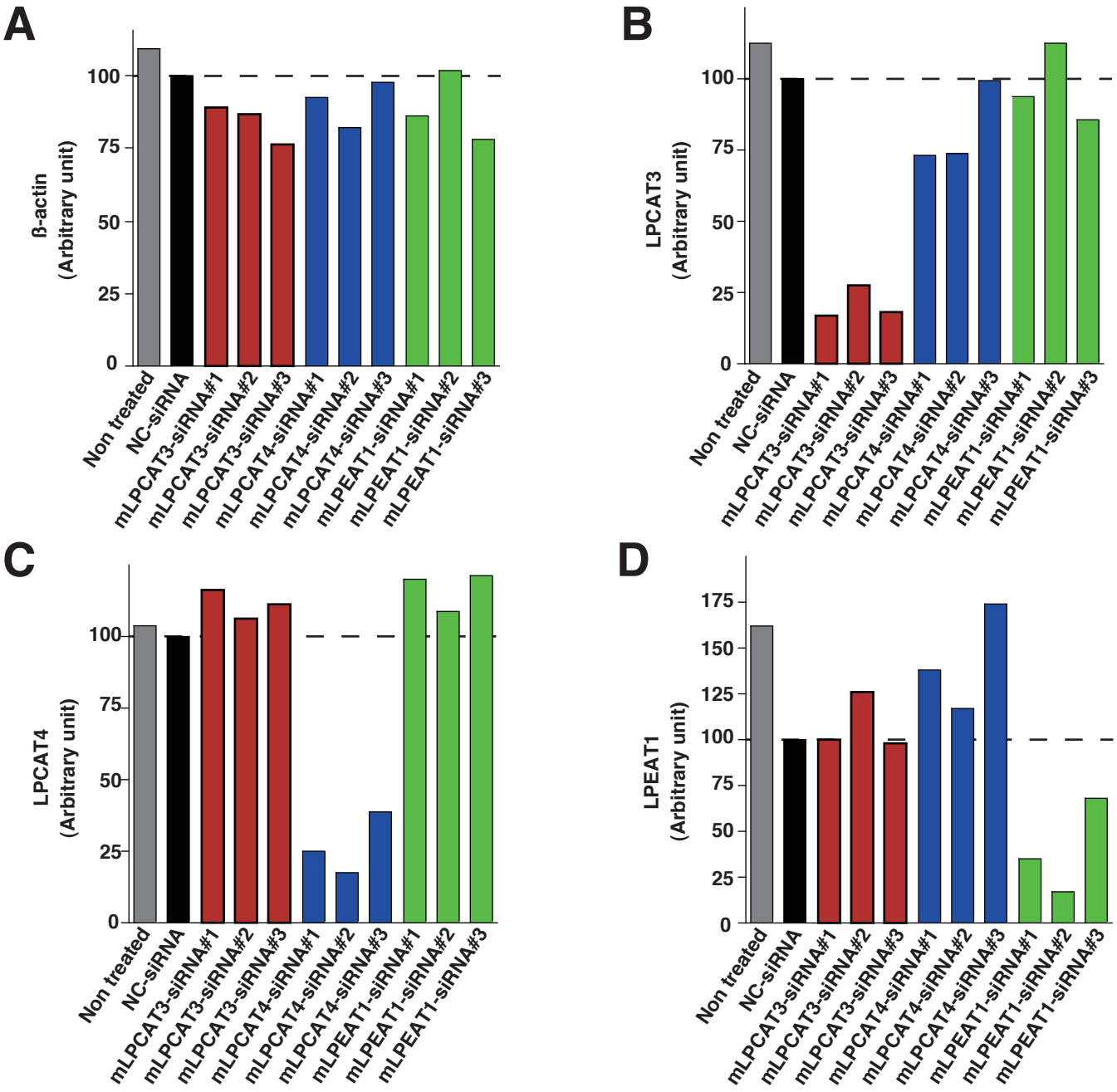

Fig. 13. Reduction of mLPCAT3, mLPCAT4, and mLPEAT1 expression by siRNA in B16 cells.

(A-D) Three siRNAs for each enzyme-siRNA and a NC-siRNA were transfected into B16 cells. After transfection for 48 h, mRNA levels of (B) mLPCAT3, (C) mLPCAT4, and (D) mLPEAT1 were reduced. (A) The mRNA of ß-actin was used as an internal control. Two independent experiments were performed with similar results.

14B), despite a reduction in the mRNA levels of mLPCAT4 and mLPEAT1 (Fig. 13C and D). In B16 cells with reduced mLPCAT3 mRNA expression, endogenous LPCAT and LPSAT activities for oleoyl-CoA were reduced compared to the control cells transfected with NC-siRNA (Fig. 14B). It is possible that mLPCAT3 and/or another unidentified LPLAT(s) compensate for LPCAT, LPEAT, and LPSAT activities in B16 cells transfected with mLPCAT4- or mLPEAT1-siRNAs, and that the expression levels of these mRNAs may be lower than that of mLPCAT3. Thus, mLPCAT3 appears to be a principal enzyme exhibiting LPCAT, LPEAT, and LPSAT activities in B16 cells. Transfection of B16 cells with mLPCAT3-, mLPCAT4-, or mLPEAT1-siRNAs did not affect LPAAT, LPGAT, or LPIAT activities (Fig.14A and B).

The effect of mLPCAT3 on phospholipid compositions as determined by LC-MS

I next analyzed the phospholipid components in the membranes of B16 cells transfected with mLPCAT3-siRNA or NC-siRNA. After exposing the cells to 10 nM arachidonic acid for 24 h, total lipids were extracted from washed cells by the Bligh-Dyer method (38) from washed cells. Lipids were analyzed using a 4000 Q-TRAP quadrupole linear ion trap hybrid mass spectrometer with an ACQUITY Ultra Performance LC. Consistent with the substrate selectivity of the enzymes determined *in vitro*, the proportion of PC, PE, and PS containing arachidonic acid (20:4) or linoleic acid (18:2) was reduced in cells transfected with mLPCAT3-siRNA transfected cells (Fig. 15B, C, E, F, H, and I). Phospholipids possessing palmitic acid (16:0) were used as a negative control (Fig. 15A, D, and G).

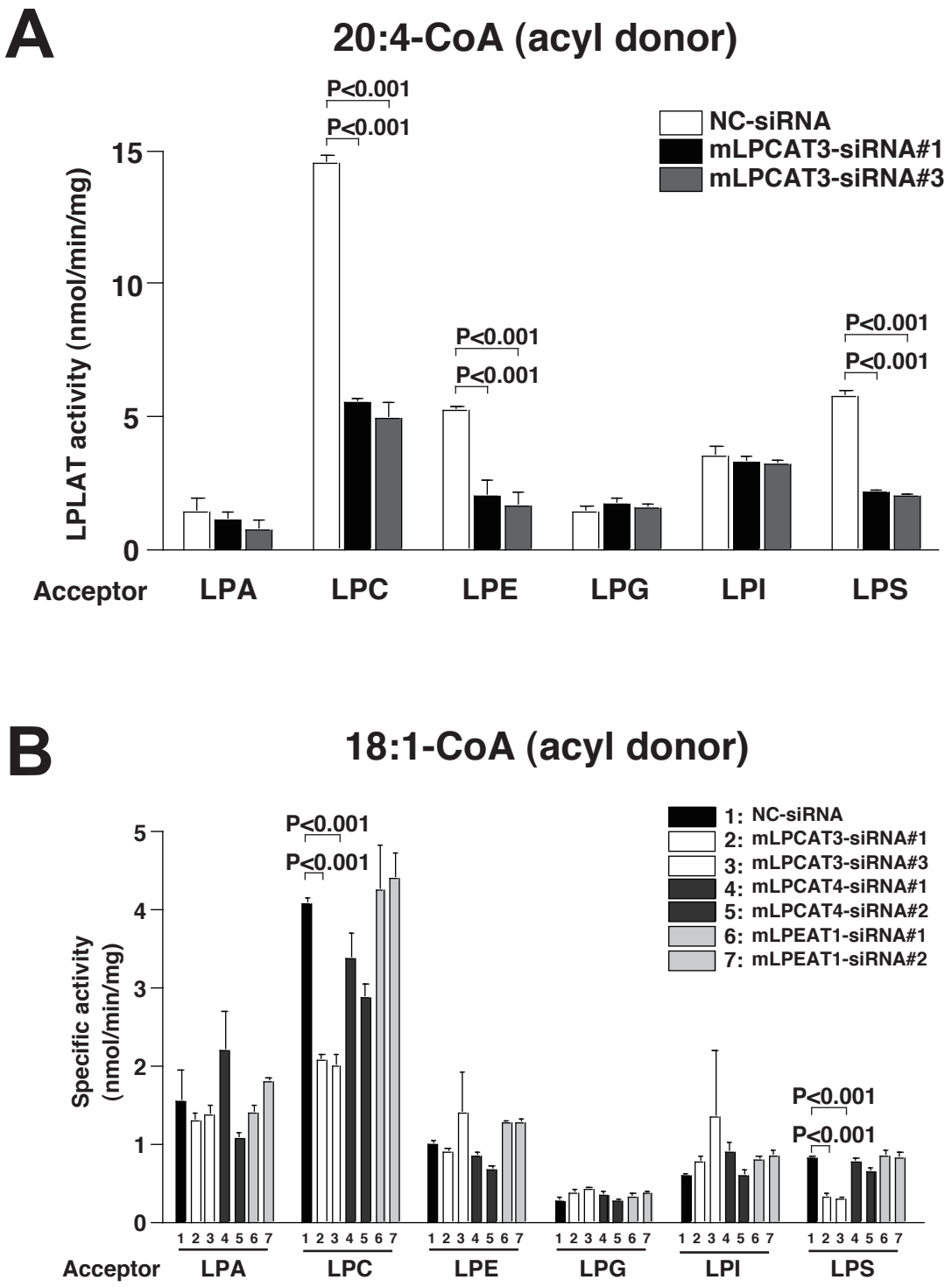

Fig. 14. Effect of the mLPCAT3, mLPCAT4, and mLPEAT1 mRNA knockdown on endogenous LPLAT activities in B16 cells.

Endogenous LPLAT activities were measured using (A) 25 μM [^{14}C]arachidonoyl-CoA or (B) 50 μM [^{14}C]oleoyl-CoA with (A) 50 μM or (B) 100 μM several lysophospholipids. The supernatants from 9,000 x *g* centrifugation were prepared from B16 cells transfected with each siRNA, and used for enzyme assays. The data represent the mean + S.D. of triplicate measurements. Two independent experiments were performed with similar results. Statistical analyses were performed by ANOVA with Tukey's Multiple Comparison test ($P < 0.001$).

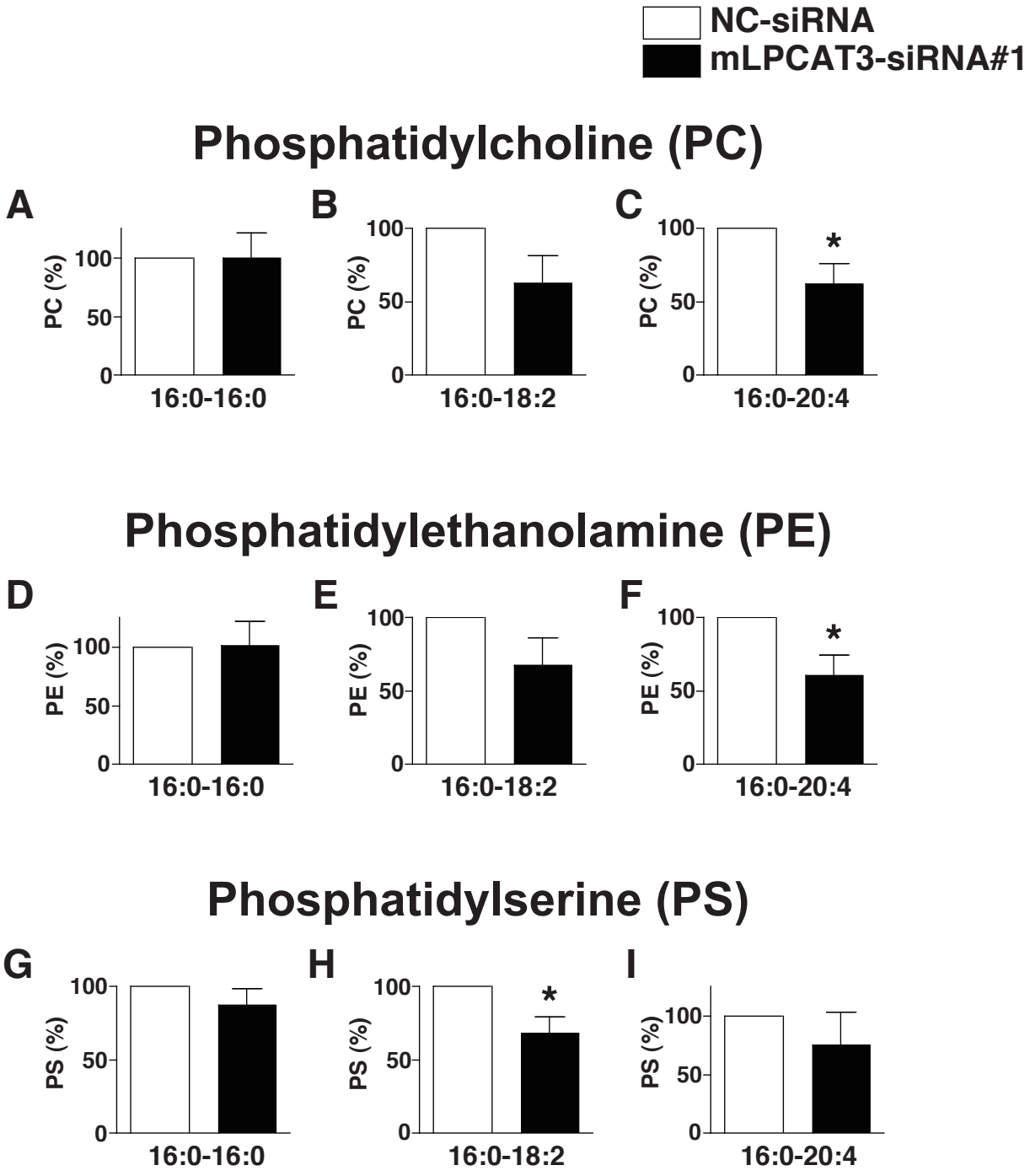

Fig. 15. Effect of mLPCAT3 knockdown on membrane phospholipid composition in B16 cells.

(A-I) The amounts of various phospholipids were measured using a 4000 Q-TRAP, as described in Materials and Methods. The levels of (A-C) PC, (D-F) PE, and (G-I) PS in B16 cells were normalized to LPC (C17:0), which was added as a control in the lipid extraction step, and the values of NC-siRNA were considered as 100%. Various lipids (*sn*-1-*sn*-2; 16:0-16:0, 16:0-18:2, and 16:0-20:4) were measured and shown. The data represent the mean + S.D. of three independent experiments. Statistical analyses were performed by one sample t test (*$P < 0.05$ versus NC-siRNA).

Discussion

Until now, the AGPAT family has been characterized as LPLATs that possessing unique LPAAT motifs. Among them, LPAATs are known to catalyze PA biosynthesis in the *de novo* pathway (Kennedy pathway), while LPGAT1, LCLAT1, LPCAT1, and LPCAT2 exert their activities in the remodeling pathway (Lands' cycle) (Fig. 1 and 2). In this study, I identified a new LPLAT family, the MBOAT family, that consists of previously reported proteins of unknown functions (35). This new LPLAT family is distinct from the AGPAT families because its members do not possess LPAAT motifs. Within this new LPLAT family, I identified novel key LPLAT enzymes, namely mLPCAT3, mLPCAT4, and mLPEAT1, which catalyze membrane phospholipid remodeling in the Lands' cycle. mLPCAT3 converted LPC, LPE, and LPS into PC, PE, and PS, respectively, using polyunsaturated fatty acyl-CoAs (18:2 and 20:4). In contrast, mLPCAT4 had LPCAT and LPEAT activities, and mLPEAT1 showed LPEAT and LPSAT activities. Both mLPCAT4 and mLPEAT1 demonstrated a clear preference for oleoyl-CoA (18:1) as an acyl donor. Importantly, mLPCAT3-siRNA mediated reduction of mLPCAT mRNA in B16 reduced the amount of PUFA containing PC, PE, and PS. This indicates that the phospholipid remodeling pathway controls the fatty acid composition of cellular phospholipids in living cells.

The MBOAT family is evolutionarily conserved from plants to mammals (35), and contains protein acyltransferases, such as Hedgehog acyltransferase (HHAT) and Porcupine that both catalyze the transfer of long-chain fatty acids (46,47). Porcupine is required for Ser209-dependent acylation (16:1) of Wnt-3a protein (already

palmitoylated at Cys77) for secretion. Hedgehog acyltransferase palmitates a Cys residue in Sonic Hedgehog, and this modification is essential for the activity of Sonic Hedgehog as well as for the generation of a protein gradient in the developing embryo. In budding yeast, the gene called GUP1 (glycerol uptake protein 1) is proposed to catalyze the remodeling of the glycosylphosphatidylinositol (GPI) anchor. MBOAT4 was identified as a ghrelin O-acyltransferase (GOAT), which esterifies Ser3 of ghrelin, an appetite-stimulating peptide hormone that contains with an octanoyl group. Acylation is important for the growth hormone releasing activity of ghrelin (48). Furthermore, acyl-CoA:cholesterol O-acyltransferase 1 (ACAT1) and ACAT2, and diacylglycerol acyltransferase 1 (DGAT1) are also included in the MBOAT family (49-52). Recently, five different research groups independently reported the identification of a budding yeast orthologue of this family as a LPLAT with most similarity to mLPCAT4 (MBOAT2) (53-57). Notably, the enzymatic properties of yeast MBOAT are different from those of mouse MBOAT. Differences in such enzymatic properties may account for the differences in membrane phospholipid composition between yeast and mammalian cells. Human MBOAT7 was recently reported as a LPIAT (58) and showed LPIAT activity with 20:4-CoA. Site-directed mutagenesis of human LPIAT1 demonstrated that a predicted active site residue, His350 within a long hydrophobic region, is important for LPIAT activity. An LPIAT1 mutant of *C. elegans* showed a “bags of worms” phenotype whereby the embryos hatched within the mother, leaving a cuticle sack that contained multiple wriggling larvae (59). Thus, the MBOAT family is comprised of enzymes that incorporate fatty acids into amino acid residues and

lysophospholipids. It is unknown which amino acid residues or motifs are important in distinguishing between lysophospholipids and proteins as acceptors.

The diversity and asymmetry of glycerophospholipids are assumed to be regulated by several PLA_2s and LPLATs that control the levels of lysophospholipids and phospholipids, which contain the precursors of lipid mediators, such as arachidonic acid at the *sn*-2 position (12,18). Arachidonic acid liberated by PLA_2s is converted into eicosanoids (12,60). Lysophospholipids constitute a different class of lipid mediators or precursors of lipid mediators, such as PAF, LPA, and the endocannabinoids (61-67). Furthermore, membrane fluidity, curvature, flexibility, and function may be partly attributed to phospholipid composition (4-6). While various types of PLA_2s have been revealed, the properties and abundance of LPLATs have not been clarified. LPLATs with a preference for different acyl-CoAs may contribute to the diversity of membrane composition, and this will be explored in the future studies. The existence of multiple LPLATs may in some way be analogous to the 20 different aminoacyl-tRNA synthetases and multiple acyltransferases that act to incorporate amino acids into preexisting polypeptides (68).

To date, numerous studies have suggested the possible presence of LPCATs, LPEATs, and LPSATs that are specific for polyunsaturated long-chain fatty acyl-CoAs (3,69-72). Recently, our group cloned and characterized two types of LPCATs, namely LPCAT1 and LPCAT2. Since LPCAT1 is highly expressed in alveolar type II cells and demonstrate selectivity, we postulated that its function is to produce pulmonary surfactant phospholipids (30,73). LPCAT2, which is mainly expressed in inflammatory

cells, is upregulated by endotoxin (a Toll-like receptor 4 agonist) stimulation in macrophages, and shows not only lysoPAF acetyltransferase activity (conversion of lysoPAF to PAF), but also LPCAT activity in the presence of Ca^{2+} (31). However, none of the activities of mLPCAT3, mLPCAT4, or mLPEAT1 were Ca^{2+}-dependent. Furthermore, innate immune agonists (Toll-like receptors 3, 4, or 9) did not induce mRNA expression of these enzymes in macrophages (Fig. 8), indicating that mLPCAT3, mLPCAT4, and mLPEAT1 play roles in membrane biogenesis in a constitutive manner. Moreover, mLPCAT3 recognizes a wide-range of acyl-CoAs, especially arachidonoyl-CoA, which is not only a major fatty acid of PC in several cell types, but also a precursor of the eicosanoids that are involved in numerous homeostatic biological functions and the inflammatory response (1,3,74). Thus, it is possible that mLPCAT3 controls the amount of eicosanoid precursors and is an important enzyme in the regulation of the remodeling pathway. Differences in phospholipid composition among various types of cells or tissues have been reported (3,75). The substrate specificities and mRNA expression patterns of these novel enzymes (LPCAT3, LPCAT4, and LPEAT1) may contribute to the production of the different varieties of membrane phospholipids seen in various tissues and thereby determine the characteristics of each cell membrane.

Interestingly, the *Drosophila* orthologue of mLPCAT3 was previously reported as *nessy*, a gene controlled by Ultrabithorax (Ubx) homeotic (Hox) and other Hox proteins during *Drosophila* embryogenesis (76). This suggests that membrane phospholipid remodeling may be important in embryogenesis, and that mLPCAT3 may

play a role in controlling the body plan by changing the phospholipid composition through the Lands' cycle. Furthermore, in a brachydactyly-syndactyly syndrome patient, human LPEAT1 located at chromosome 6 is disrupted (77), suggesting that human LPEAT1 contributes to the turnover of phospholipids for normal development and organogenesis. Importantly, it is known that the LPLAT activity is known to be affected by the inflammatory cytokines such as Interferon-γ. Thus, LPLATs are considered as a new target for the drug discovery (45).

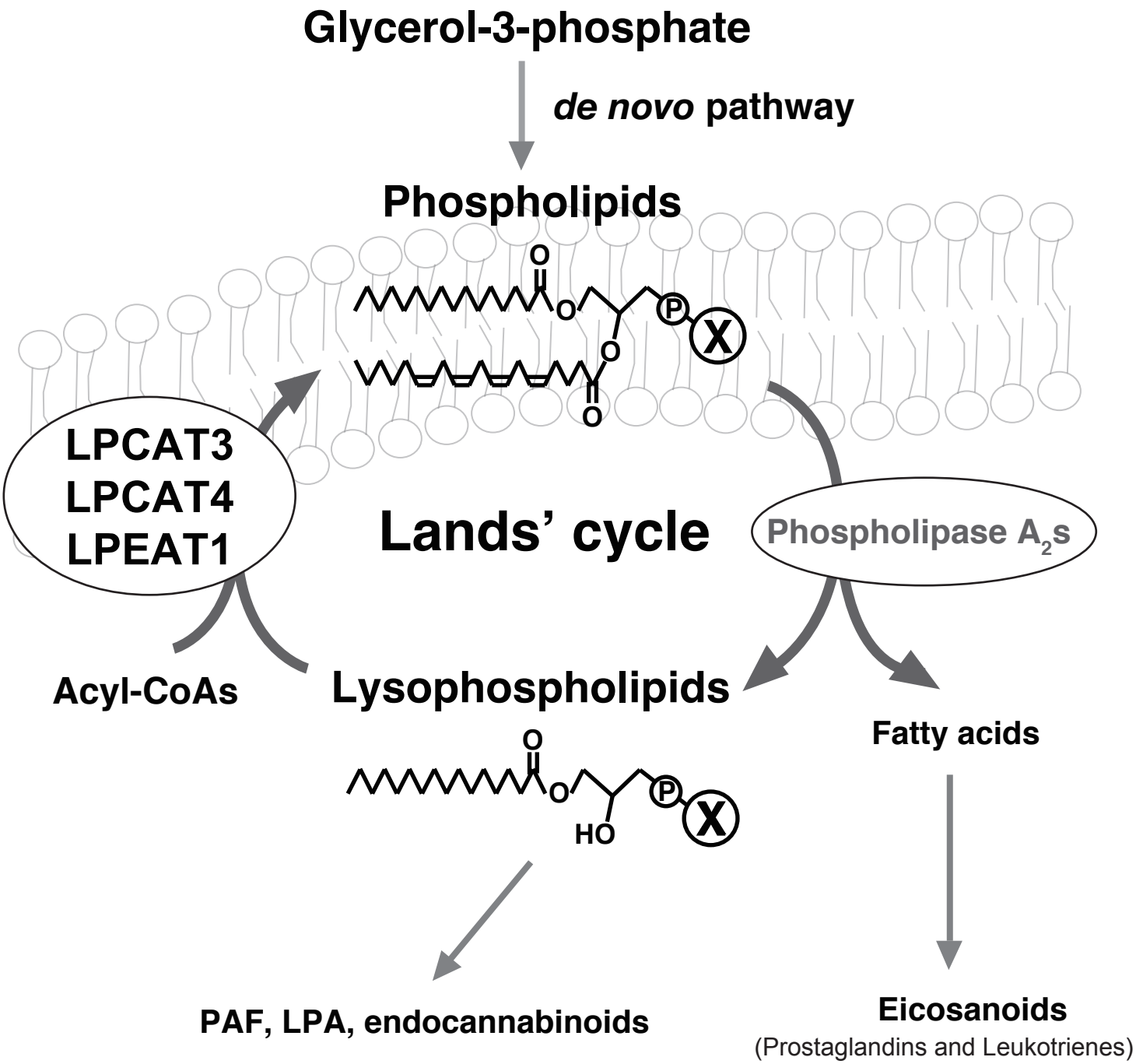

Fig. 16. Summary of this study.

In this study, I identified and characterized three new LPLATs (LPCAT3, LPCAT4, and LPEAT1) witch is important for the reacylation of lysophospholipids in Lands' cycle.

Conclusion

I have identified a novel LPLAT family, named MBOAT family, which consists of three novel LPLATs, i.e. LPCAT3, LPCAT4, and LPEAT1. These enzymes of MBOAT family contribute to membrane biogenesis and diversity (Fig. 16). Further studies are needed to elucidate the roles of mLPCAT3, mLPCAT4, and mLPEAT1 *in vivo*, and to determine their potential as novel therapeutic targets in various diseases. To date, the study of membrane biogenesis in the remodeling pathway (i.e. the Lands' cycle) has been delayed due to the lack of information about the key enzymes involved. Discovery of this new LPLAT family paves the way for a better understanding of membrane asymmetry and diversity.

References

1. Wood, R., and Harlow, R. D. (1969) *Arch Biochem Biophys* **135**(1), 272-281
2. Schlame, M., Brody, S., and Hostetler, K. Y. (1993) *Eur J Biochem* **212**(3), 727-735
3. Yamashita, A., Sugiura, T., and Waku, K. (1997) *J Biochem (Tokyo)* **122**(1), 1-16
4. Stubbs, C. D., and Smith, A. D. (1984) *Biochim Biophys Acta* **779**(1), 89-137
5. van Meer, G. (2005) *Embo J* **24**(18), 3159-3165
6. van Meer, G., and Vaz, W. L. (2005) *EMBO Rep* **6**(5), 418-419
7. Kornberg, A., and Pricer, W. E., Jr. (1953) *J Biol Chem* **204**(1), 345-357
8. Gimeno, R. E., and Cao, J. (2008) *J Lipid Res* **49**, 2079-2088
9. Kennedy, E. P., and Weiss, S. B. (1956) *J Biol Chem* **222**(1), 193-214
10. Kume, K., and Shimizu, T. (1997) *Biochem Biophys Res Commun* **237**(3), 663-666
11. Vance, J. E., and Vance, D. E. (2004) *Biochem Cell Biol* **82**, 113-128
12. Nakagawa, Y., and Waku, K. (1989) *Prog Lipid Res* **28**(3), 205-243
13. Farooqui, A. A., Horrocks, L. A., and Farooqui, T. (2000) *Chem Phys Lipids* **106**(1), 1-29
14. Shimizu, T. (2008) *Annu Rev Pharmacol Toxicol*
15. Shindou, H., and Shimizu, T. (2008) *J Biol Chem*

16. Shindou, H., Hishikawa, D., Harayama, T., Yuki, K., and Shimizu, T. (2008) *J Lipid Res*

17. Lands, W. E. (1958) *J Biol Chem* **231**(2), 883-888

18. Shimizu, T., Ohto, T., and Kita, Y. (2006) *IUBMB Life* **58**(5-6), 328-333

19. Dawson, R. M. (1978) *Adv Exp Med Biol* **101**, 1-13

20. Farooqui, A. A., Yang, H. C., Rosenberger, T. A., and Horrocks, L. A. (1997) *J Neurochem* **69**(3), 889-901

21. Asai, K., Hirabayashi, T., Houjou, T., Uozumi, N., Taguchi, R., and Shimizu, T. (2003) *J Biol Chem* **278**(10), 8809-8814

22. Eberhardt, C., Gray, P. W., and Tjoelker, L. W. (1997) *J Biol Chem* **272**(32), 20299-20305

23. Hollenback, D., Bonham, L., Law, L., Rossnagle, E., Romero, L., Carew, H., Tompkins, C. K., Leung, D. W., Singer, J. W., and White, T. (2006) *J Lipid Res* **47**(3), 593-604

24. Li, D., Yu, L., Wu, H., Shan, Y., Guo, J., Dang, Y., Wei, Y., and Zhao, S. (2003) *J Hum Genet* **48**(8), 438-442

25. Cao, J., Liu, Y., Lockwood, J., Burn, P., and Shi, Y. (2004) *J Biol Chem* **279**(30), 31727-31734

26. Yang, Y., Cao, J., and Shi, Y. (2004) *J Biol Chem* **279**(53), 55866-55874

27. Lu, B., Jiang, Y. J., Zhou, Y., Xu, F. Y., Hatch, G. M., and Choy, P. C. (2005) *Biochem J* **385**(Pt 2), 469-477

28. Ye, G. M., Chen, C., Huang, S., Han, D. D., Guo, J. H., Wan, B., and Yu, L. (2005) *DNA Seq* **16**(5), 386-390

29. Xu, Y., Malhotra, A., Ren, M., and Schlame, M. (2006) *J Biol Chem* **281**(51), 39217-39224

30. Nakanishi, H., Shindou, H., Hishikawa, D., Harayama, T., Ogasawara, R., Suwabe, A., Taguchi, R., and Shimizu, T. (2006) *J Biol Chem* **281**(29), 20140-20147

31. Shindou, H., Hishikawa, D., Nakanishi, H., Harayama, T., Ishii, S., Taguchi, R., and Shimizu, T. (2007) *J Biol Chem* **282**(9), 6532-6539

32. Lewin, T. M., Wang, P., and Coleman, R. A. (1999) *Biochemistry* **38**(18), 5764-5771

33. Shikano, S., and Li, M. (2003) *Proc Natl Acad Sci U S A* **100**(10), 5783-5788

34. MacDonald, J. I., and Sprecher, H. (1991) *Biochim Biophys Acta* **1084**(2), 105-121

35. Hofmann, K. (2000) *Trends Biochem Sci* **25**(3), 111-112

36. Niwa, H., Yamamura, K., and Miyazaki, J. (1991) *Gene* **108**(2), 193-199

37. Bradford, M. M. (1976) *Anal Biochem* **72**, 248-254

38. Bligh, E. G., and Dyer, W. J. (1959) *Can J Biochem Physiol* **37**(8), 911-917

39. Houjou, T., Yamatani, K., Nakanishi, H., Imagawa, M., Shimizu, T., and Taguchi, R. (2004) *Rapid Commun Mass Spectrom* **18**(24), 3123-3130

40. Thompson, J. D., Higgins, D. G., and Gibson, T. J. (1994) *Nucleic Acids Res* **22**(22), 4673-4680

41. Tusnady, G. E., and Simon, I. (2001) *Bioinformatics* **17**(9), 849-850

42. Snapp, E. L., Hegde, R. S., Francolini, M., Lombardo, F., Colombo, S., Pedrazzini, E., Borgese, N., and Lippincott-Schwartz, J. (2003) *J Cell Biol* **163**(2), 257-269

43. Tou, J. S. (1987) *Lipids* **22**, 333-337

44. Jackson, S. K. (1997) *Prog Lipid Res* **36**, 227-244

45. Jackson, S. K., Abate, W., and Tonks, A. J. (2008) *Pharmacol Ther* **119**(1), 104-114

46. Chen, M. H., Li, Y. J., Kawakami, T., Xu, S. M., and Chuang, P. T. (2004) *Genes Dev* **18**(6), 641-659

47. Takada, R., Satomi, Y., Kurata, T., Ueno, N., Norioka, S., Kondoh, H., Takao, T., and Takada, S. (2006) *Dev Cell* **11**(6), 791-801

48. Yang, J., Brown, M. S., Liang, G., Grishin, N. V., and Goldstein, J. L. (2008) *Cell* **132**(3), 387-396

49. Chang, C. C., Huh, H. Y., Cadigan, K. M., and Chang, T. Y. (1993) *J Biol Chem* **268**(28), 20747-20755

50. Oelkers, P., Behari, A., Cromley, D., Billheimer, J. T., and Sturley, S. L. (1998) *J Biol Chem* **273**(41), 26765-26771

51. Anderson, R. A., Joyce, C., Davis, M., Reagan, J. W., Clark, M., Shelness, G. S., and Rudel, L. L. (1998) *J Biol Chem* **273**(41), 26747-26754

52. Cases, S., Smith, S. J., Zheng, Y. W., Myers, H. M., Lear, S. R., Sande, E., Novak, S., Collins, C., Welch, C. B., Lusis, A. J., Erickson, S. K., and Farese, R. V., Jr. (1998) *Proc Natl Acad Sci U S A* **95**(22), 13018-13023

53. Riekhof, W. R., Wu, J., Jones, J. L., and Voelker, D. R. (2007) *J Biol Chem* **282**(39), 28344-28352

54. Jain, S., Stanford, N., Bhagwat, N., Seiler, B., Costanzo, M., Boone, C., and Oelkers, P. (2007) *J Biol Chem* **282**(42), 30562-30569

55. Benghezal, M., Roubaty, C., Veepuri, V., Knudsen, J., and Conzelmann, A. (2007) *J Biol Chem* **282**(42), 30845-30855

56. Tamaki, H., Shimada, A., Ito, Y., Ohya, M., Takase, J., Miyashita, M., Miyagawa, H., Nozaki, H., Nakayama, R., and Kumagai, H. (2007) *J Biol Chem* **282**(47), 34288-34298

57. Chen, Q., Kazachkov, M., Zheng, Z., and Zou, J. (2007) *FEBS Lett* **581**, 5511-5516

58. Matsuda, S., Inoue, T., Lee, H. C., Kono, N., Tanaka, F., Gengyo-Ando, K., Mitani, S., and Arai, H. (2008) *Genes Cells* **13**(8), 879-888

59. Lee, H. C., Inoue, T., Imae, R., Kono, N., Shirae, S., Matsuda, S., Gengyo-Ando, K., Mitani, S., and Arai, H. (2008) *Mol Biol Cell* **19**, 1174-1184

60. Narumiya, S., Sugimoto, Y., and Ushikubi, F. (1999) *Physiol Rev* **79**(4), 1193-1226

61. Samuelsson, B., Dahlen, S. E., Lindgren, J. A., Rouzer, C. A., and Serhan, C. N. (1987) *Science* **237**(4819), 1171-1176

62. Fukushima, N., Kimura, Y., and Chun, J. (1998) *Proc Natl Acad Sci U S A* **95**(11), 6151-6156

63. Ishii, S., and Shimizu, T. (2000) *Prog Lipid Res* **39**(1), 41-82

64. Hla, T., Lee, M. J., Ancellin, N., Paik, J. H., and Kluk, M. J. (2001) *Science* **294**(5548), 1875-1878

65. Wang, L., Liu, J., Harvey-White, J., Zimmer, A., and Kunos, G. (2003) *Proc Natl Acad Sci U S A* **100**(3), 1393-1398

66. Prescott, S. M., Zimmerman, G. A., Stafforini, D. M., and McIntyre, T. M. (2000) *Annu Rev Biochem* **69**, 419-445

67. Haeggstrom, J. Z., and Wetterholm, A. (2002) *Cell Mol Life Sci* **59**(5), 742-753

68. Ibba, M., and Soll, D. (2000) *Annu Rev Biochem* **69**, 617-650

69. Waku, K., and Lands, W. E. (1968) *J Lipid Res* **9**(1), 12-18

70. Okuyama, H., Eibl, H., and Lands, W. E. (1971) *Biochim Biophys Acta* **248**(2), 263-273

71. Holub, B. J. (1980) *Biochim Biophys Acta* **618**(2), 255-262

72. Masuzawa, Y., Sugiura, T., Sprecher, H., and Waku, K. (1989) *Biochim Biophys Acta* **1005**(1), 1-12

73. Chen, X., Hyatt, B. A., Mucenski, M. L., Mason, R. J., and Shannon, J. M. (2006) *Proc Natl Acad Sci U S A* **103**(31), 11724-11729

74. Funk, C. D. (2001) *Science* **294**(5548), 1871-1875

75. Kuksis, A., Breckenridge, W. C., Marai, L., and Stachnyk, O. (1969) *J Lipid Res* **10**(1), 25-32

76. Maurel-Zaffran, C., Chauvet, S., Jullien, N., Miassod, R., Pradel, J., and Aragnol, D. (1999) *Mech Dev* **86**(1-2), 159-163

77. Dauwerse, J. G., de Vries, B. B., Wouters, C. H., Bakker, E., Rappold, G., Mortier, G. R., Breuning, M. H., and Peters, D. J. (2007) *Eur J Hum Genet* **15**(7), 743-751

Acknowledgements

I would like to express my gratitude to all of those who gave me the opportunity to complete this thesis. I am deeply indebted to my supervisors, Prof. Takao Shimizu and Dr. Hideo Shindou, whose advise, support, stimulating suggestions and encouragement helped me throughout the course of my Ph.D. program. I also thank Prof. Ryo Taguchi and Mr. Hiroki Nakanishi at Department of Metabolome, the University of Tokyo, who provided me with instructions for experiments and with scientific suggestions. I am grateful to all of the members in my laboratory for their encouragement and support. Finally, I would like to thank my family for endless affection and support all along the way.